AD_____

Award Number:
W81XWH-12-1-0438

TITLE:
The Role of Mesenchymal Stem Cells in Promoting Ovarian Cancer Growth and Spread

PRINCIPAL INVESTIGATOR:
Aline M. Betancourt, PhD

CONTRACTING ORGANIZATION:
Tulane University
New Orleans, LA 70112

REPORT DATE:
September 2013

TYPE OF REPORT: **Annual report**

PREPARED FOR: U.S. Army Medical Research and Materiel Command
Fort Detrick, Maryland 21702-5012

DISTRIBUTION STATEMENT: Approved for Public Release;
Distribution Unlimited

The views, opinions and/or findings contained in this report are those of the author(s) and should not be construed as an official Department of the Army position, policy or decision unless so designated by other documentation.

REPORT DOCUMENTATION PAGE

Form Approved
OMB No. 0704-0188

Public reporting burden for this collection of information is estimated to average 1 hour per response, including the time for reviewing instructions, searching existing data sources, gathering and maintaining the data needed, and completing and reviewing this collection of information. Send comments regarding this burden estimate or any other aspect of this collection of information, including suggestions for reducing this burden to Department of Defense, Washington Headquarters Services, Directorate for Information Operations and Reports (0704-0188), 1215 Jefferson Davis Highway, Suite 1204, Arlington, VA 22202-4302. Respondents should be aware that notwithstanding any other provision of law, no person shall be subject to any penalty for failing to comply with a collection of information if it does not display a currently valid OMB control number. **PLEASE DO NOT RETURN YOUR FORM TO THE ABOVE ADDRESS.**

1. REPORT DATE
September 2013

2. REPORT TYPE
Annual Report

3. DATES COVERED
01 Sepember 2012 to 31 August 2013

4. TITLE AND SUBTITLE
The Role of Mesenchymal Stem Cells in Promoting Ovarian Cancer Growth and Spread

5a. CONTRACT NUMBER

5b. GRANT NUMBER
W81XWH-12-1-0438

5c. PROGRAM ELEMENT NUMBER

5d. PROJECT NUMBER

5e. TASK NUMBER

5f. WORK UNIT NUMBER

6. AUTHOR(S)
Aline M. Betancourt, PhD

E-Mail: alibscan@tulane.edu

7. PERFORMING ORGANIZATION NAME(S) AND ADDRESS(ES)
Tulane University
New Orleans, LA 70112

8. PERFORMING ORGANIZATION REPORT NUMBER

9. SPONSORING / MONITORING AGENCY NAME(S) AND ADDRESS(ES)
U.S. Army Medical Research and Materiel Command
Fort Detrick, Maryland 21702-5012

10. SPONSOR/MONITOR'S ACRONYM(S)

11. SPONSOR/MONITOR'S REPORT NUMBER(S)

12. DISTRIBUTION / AVAILABILITY STATEMENT
Approved for Public Release; Distribution Unlimited

13. SUPPLEMENTARY NOTES

14. ABSTRACT

Despite more than three decades of therapies that selectively target the tumor cells, the 5-year survival rate for metastatic ovarian cancer patients remains at less than 30%. New strategies that can change this dismal scenario are urgently needed to improve or complement classical treatments for this malignancy. Targeting the tumor microenvironment (TME) represents one such new therapeutic strategy. Tumors depend on a supportive microenvironment to thrive and disseminate. Experimental clinical strategies that target the ovarian tumor microenvironment are beginning to show some promise. Mesenchymal stem cells (MSCs) are known to reside in TME or tumor stroma. Therefore, gene-modified MSCs that can act as "Trojan horses" and deliver anti-cancer therapeutics into the tumor stroma are being evaluated as a promising new specific cell-based therapy for cancer.

We established that MSCs promoted ovarian tumor growth. We have also developed new methodology to induce the standard mixed pool of MSCs into two uniform but distinct phenotypes, *MSC1* and *MSC2*. In recent studies we found that when we delivered *MSC2* into mouse models of ovarian cancer, tumors grew and spread faster. Whereas surprisingly when we delivered *MSC1* into the mice there was an opposite anti-tumor effect. We do not yet know the mechanisms behind this *MSC1* mediated inhibition of tumor growth.

15. SUBJECT TERMS
BMSC, bone marrow-derived mesenchymal stem cell, MSC, mesenchymal stem cell, MSC1, pro-inflammatory phenotype, MSC2, anti-inflammatory phenotype

16. SECURITY CLASSIFICATION OF:			**17. LIMITATION OF ABSTRACT**	**18. NUMBER OF PAGES**	**19a. NAME OF RESPONSIBLE PERSON**
a. REPORT	**b. ABSTRACT**	**c. THIS PAGE**			USAMRMC
U	U	U	UU		**19b. TELEPHONE NUMBER** *(include area code)*

Table of Contents

	Page
**Introduction……..……..…..	**4**
**Body……..	**5-9**
**Key Research Accomplishments…….……..	**10**
**Reportable Outcomes……	**11-12**
**Conclusion……	**13**
**References…….	**14**
**Appendices……	**15-26**

INTRODUCTION:

o **Background:** Currently, there are many promising clinical trials using mesenchymal stem cells (MSCs) in cell-based therapies of diseases ranging widely from graft-versus-host to joint and cartilage disorders. Increasingly, however, there is a concern over the clinical use of MSCs because they are also known to home to tumors and once resident in the tumor microenvironment (TME) to support tumor growth and spread. For instance, we established that MSCs in the ovarian tumor microenvironment promoted tumor growth and favored angiogenesis. We also developed new methodology to induce the standard mixed pool of MSCs into two uniform but distinct phenotypes, *MSC1* and *MSC2*. In recent studies we found that *MSC2* supported ovarian cancer growth and spread while surprisingly *MSC1* had an opposite anti-tumor effect. We do not yet know the mechanisms behind this *MSC1* mediated inhibition of tumor growth.

o **Objective/Hypothesis:** Our *long-term goal* is to determine the role that MSCs play in cancer growth and spread in order to design more effective tumor therapies. The *objective here* is to establish whether induction of MSCs into *MSC1* is a feasible new anti-tumor cell-based therapy approach, and to identify the molecular mechanisms behind the *MSC1* mediated anti-tumor effect. Our *central hypothesis* is that *MSC1* will home to the ovarian tumor microenvironment and shift the balance from a tumor promoting stroma to a tumor eradicating one that attenuates tumor growth and spread by influencing the secretion of defined soluble factors and extracellular matrix proteins as well as modifying the host immune response.

o **Specific Aims:**
Aim 1. Determine the effect of MSC-based therapies on ovarian tumor growth and spread.
Aim 2. Determine the anti-tumor mechanisms established by MSC1-treatment of MOSEC mice.

o **Study Design:**
Aim 1. Determine the effect of MSC-based therapies on ovarian tumor growth and spread. We will test the *hypothesis* that *MSC1*-based therapy can effectively attenuate ovarian tumor growth and spread in an established immune competent model (MOSEC) when compared to MSCs- or vehicle-treated animals. MSC engraftment, tumor growth and spread, as well as survival data will be collected.

Aim 2. Determine the anti-tumor mechanisms established by MSC1-treatment of MOSEC mice. The effect on TME and systemic immune and inflammatory responses will be evaluated. Changes in the secretion of inflammatory factors, ECM, and immune cells will be measured from the ovarian TME, ascites, draining lymph nodes and spleen of mice treated with standard MSCs, *MSC1*, or vehicle controls.

o **Impact:**

Our objectives in this TEAL Expansion award study are to show that *MSC1*-based therapy attenuates tumor growth and spread in a murine ovarian cancer model and to identify the specific *MSC1*-therapy driven anti-tumor mechanisms. This approach has the potential to identify new targets for preventive and therapeutic interventions of ovarian cancer, as well as to determine the contributions of stromal components to ovarian cancer growth and spread. We also expect that by identifying the mechanisms behind the divergent tumor effects of conventional MSCs and *MSC1*, we will shed some light on the growing controversy over whether MSCs are safe in cell-based therapies of human disease. Therefore, these studies should lay the groundwork for safe cell-based therapies that inhibit tumor growth and spread.

BODY:

We have included the study as it was described in our Statement of Work and following each section presented what we have accomplished based on the proposed work.

Statement of Work

Goals and Objectives: Our *long-term goal* is to determine the role that MSCs play in cancer growth and spread in order to design more effective tumor therapies. The *objective here* is to establish whether induction of MSCs into *MSC1* is a feasible new anti-tumor cell-based therapy approach, and to identify the molecular mechanisms behind the *MSC1* mediated anti-tumor effect. Our central hypothesis is that *MSC1* will home to the ovarian tumor microenvironment and shift the balance from a tumor promoting stroma to a tumor eradicating one that attenuates tumor growth and spread by influencing the secretion of defined soluble factors and extracellular matrix proteins as well as modifying the host immune response.

Task 0. **Obtain IACUC and ACURO approval for this project**. (before start of project) COMPLETED

Task 1. **Determine the effect of MSC-based therapies on ovarian tumor growth and spread** (Months 1-12):

A. *Optimal MSC1 Treatment Regimen.* The murine ovarian surface epithelia carcinoma (MOSEC) inoculated mice or MOSEC model will be treated intraperitonealy (IP) with MSCs ($1x10^6$ cells), *MSC1* ($1x10^6$ cells), or vehicle weekly for 3 weeks. The first group of mice will start MSC treatments at day 15 (pre-clinical disease). Group 2 will start MSC treatment at day 20 (early disease). Group 3 will start at day 30 (established disease). Mice will be monitored every other day until termination at day 75. (Months 1-6, 108 C57Bl/6J mice)

Group	Day of MSC-tx	Vehicle Control	MSCs	MSC1
1	15 (pre-clinical disease)	2	8	8
2	20 (early disease)	2	8	8
3	30 (established Disease)	2	8	8

Vehicle control mice will receive IP injections with HBSS (0.1mL). MSCs-are animals that will receive MSCs prepared by standard unmodified methodology, *MSC1-* animals receive MSCs primed by our methodology into a uniform phenotype, respectively. One animal from each group will be harvested 24hrs after the final MSC-treatment to track the fate of the MSCs in the animals. All other animals will be harvested at day 75. MOSEC mice will be treated intraperitonealy (IP) with MSCs ($1x10^6$ cells), *MSC1* ($1x10^6$ cells), or vehicle on day 30. The first group of MOSEC mice will start MSC treatments at day 15 (pre-clinical disease). Group 2 will start MSC treatment at day 20 (early disease). Group 3 will start at day 30 (established disease). Mice will be monitored every other day until termination at day 75. Cell number and treatment days selected was guided by previous studies Coffelt *et al.*, 2009). Data will be presented as survival plots (log rank tests), tumor volume changes over time, number of metastasized tumors, and micrographs of tumor sections. This experiment will require a total of 54 animals. Since 2 donors will be tested a total of **108 animals** will be needed.

Task 1.A COMPLETED

Unpublished Experimental Results

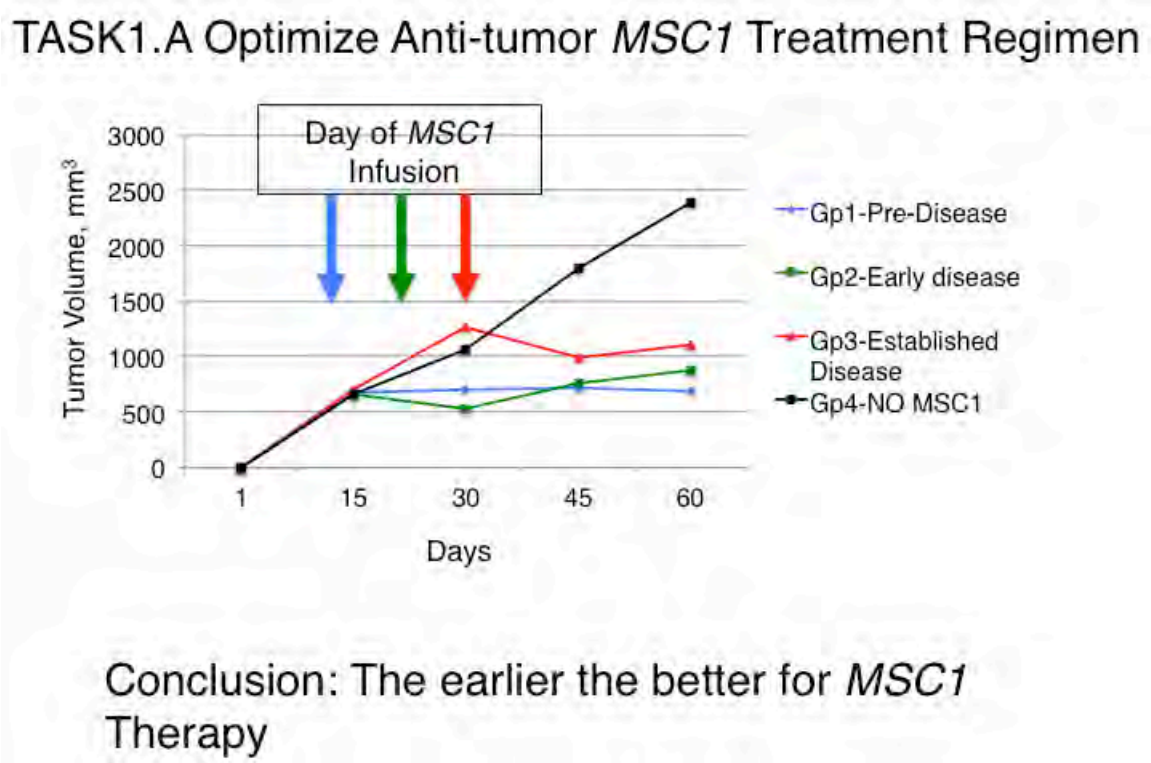

Following figure legend:
The murine ovarian surface epithelia carcinoma (MOSEC) inoculated mice or MOSEC model was treated intraperitonealy (IP) with a single injection of anti-tumor MSC1 as indicated by the arrows ↓ with colors matching their corresponding group. MOSEC mice were infused with *MSC1* ($1x10^6$ cells), or vehicle (Gp4). The first group of MOSEC mice had MSC1 treatment at day 15 (pre-clinical disease). Group 2 was treated with MSC1 at day 20 (early disease). Group 3 was treated at day 30 (established disease). Mice were monitored every other day until termination at day 60. Tumor growth was measured at weekly intervals until day of mouse sacrifice (Day 60). Harvested tumors and metastasis were weighed, counted and processed. Accumulated ascites was collected, measured, and a sample was spun on cytospin slides and stained by DiffQuick cytology stain by standard methods. Gp. 1 (2 mL), 2 (1.5 mL) and 3 (5mL) had accumulated some ascites. Gp4 the untreated control animals had more ascites(>10mL) and enlarged spleens, respectively. The average +/-SEM is reported in fig. with at least 5 mice per treatment group. The average +/-SEM is reported in fig. with at least 5 mice per treatment group.

B. *Optimal MSC Cell Number*. The mice will be treated IP with MSCs, *MSC1*, or vehicle weekly for 3 weeks starting on the optimal treatment day (determined above). Group 1 will be treated with 250,000 cells. Group 2 through 4 will be treated with 500,000, 1 $x10^6$, or 2 $x10^6$ cells, respectively. Group 5 will be treated with vehicle as control. Mice will be monitored weekly until termination at day 75. (Months 1-6, 144 C57Bl/6J mice)

Group	Number of MSCs delivered	Vehicle Control	MSCs	MSC1
1	250K	-	8	8
2	500K	-	8	8
3	$1x10^6$	-	8	8
4	$2x10^6$	-	8	8
5	0	8	-	-

The MOSEC mice will be treated intraperitonealy (IP) with MSCs, *MSC1*, or vehicle on the optimal treatment day determined above. Group 1 will be treated with 250,000 cells. Group 2 through 4 will be treated with 500,000, 1 $x10^6$, or 2 $x10^6$ cells, respectively. Group 5 will be treated with vehicle as control. Mice will be monitored every other day until termination at day 75. Data will be presented as above. This experiment will require a total of 72 animals. Since 2 donors will be tested a total of **144 animals** will be needed.

Task 1.B COMPLETED

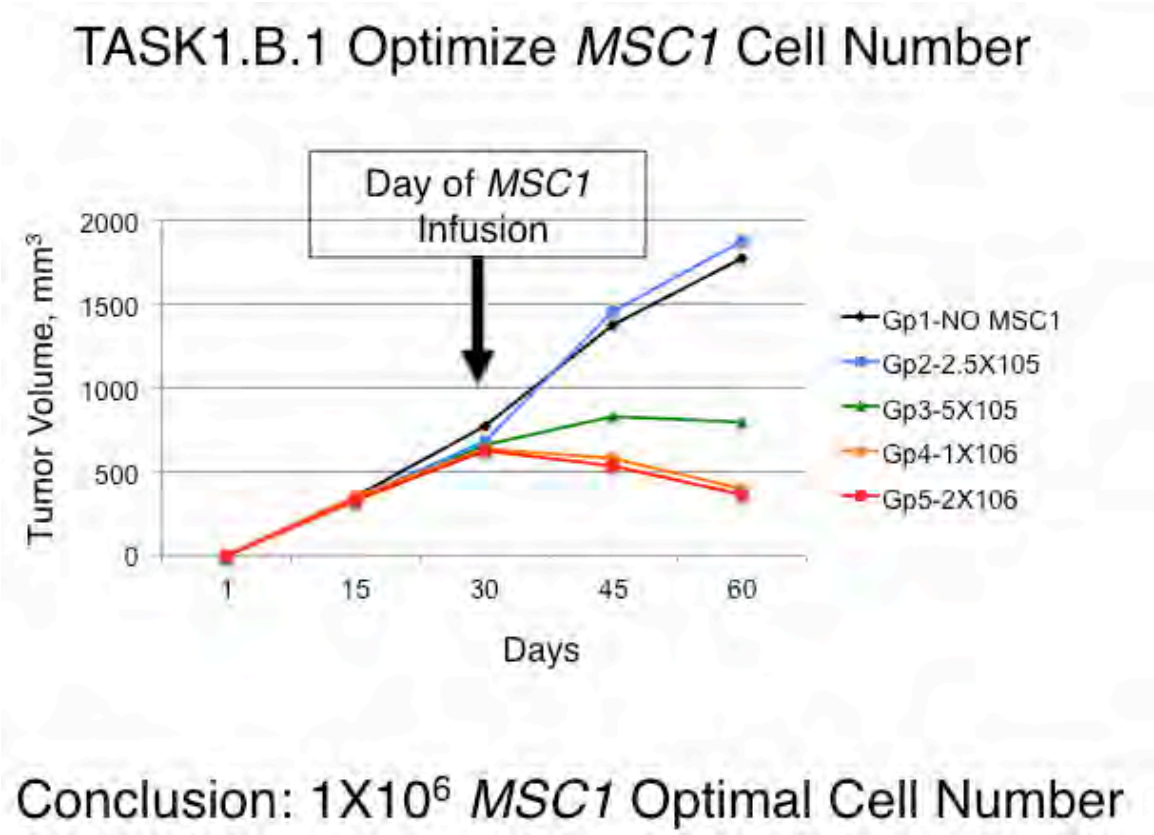

Unpublished Experimental Results

Following figure legend:
The murine ovarian surface epithelia carcinoma (MOSEC) inoculated mice or MOSEC model was treated intraperitonealy (IP) with a

single injection of anti-tumor MSC1 as indicated by the black arrow ↓. Group 1 was treated with vehicle as control. Group 2 was treated with 250,000 cells. Group 3 through 5 was treated with 500,000, 1 x10^6, or 2 x10^6 cells, respectively. Tumor growth was measured at weekly intervals until day of mouse sacrifice (Day 60). Harvested tumors and metastasis were weighed, counted and processed. Accumulated ascites was collected, measured, and a sample was spun on cytospin slides and stained by DiffQuick cytology stain by standard methods. Gp. 1 (10mL), 2 (10mL) and 3 (1.5mL) had accumulated ascites and enlarged spleens, respectively. The average +/-SEM is reported in fig. with at least 5 mice per treatment group.

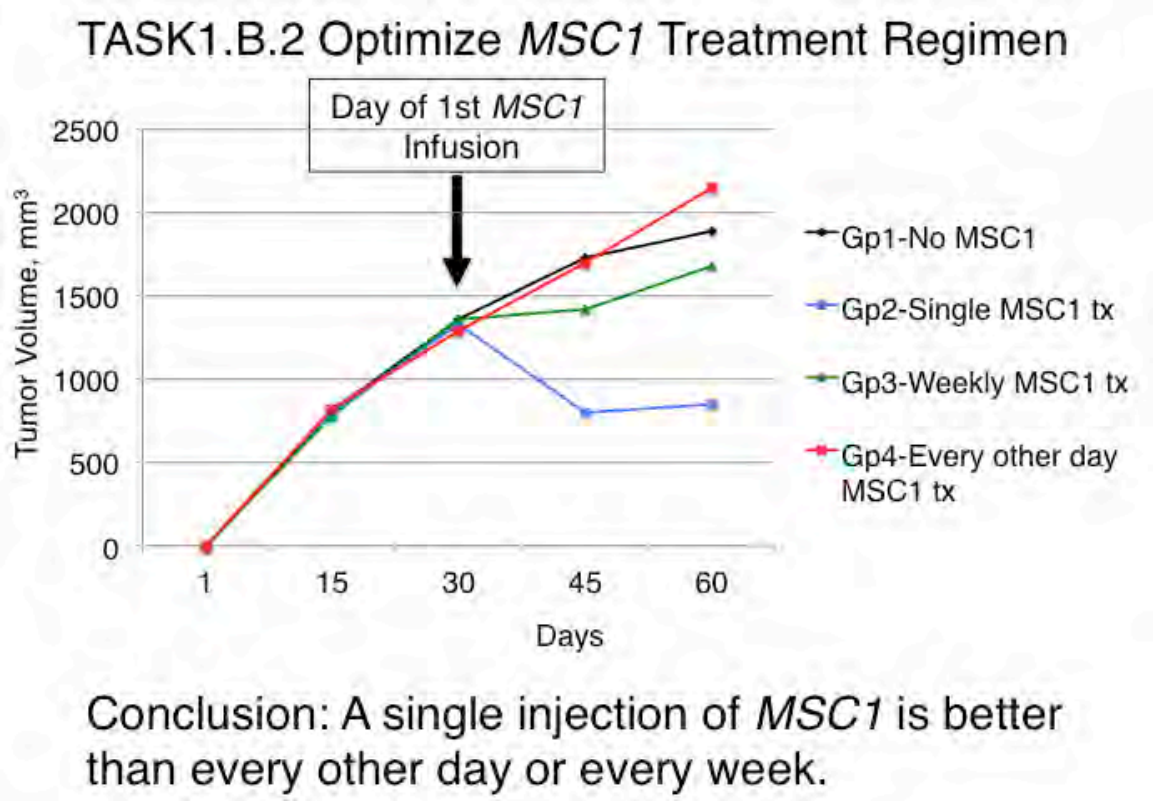

Following figure legend:
The murine ovarian surface epithelia carcinoma (MOSEC) inoculated mice or MOSEC model was treated intraperitonealy (IP) with anti-tumor *MSC1* starting on day 30 as indicated by the black arrow ↓. Group 1 was treated with vehicle as control. Group 2 was treated with a single anti-tumor *MSC1* injection (1 x10^6). Group 3 was treated with weekly anti-tumor *MSC1* injections of 1 x10^6 cells starting on day 30. Group 4 was treated with anti-tumor *MSC1* (1 x10^6 cells) every other day. Tumor growth was measured at weekly intervals until day of mouse sacrifice (Day 60). Harvested tumors and metastasis were weighed, counted and processed. Accumulated ascites was collected, measured, and a sample was spun on cytospin slides and stained by DiffQuick cytology stain by standard methods. Surprisingly, Gp3 (>10mL) and Gp4 (>10mL) animals had worse disease and more ascites than even the untreated control Gp1 (10mL). Consistent with previous experiments a single *MSC1* infusion led to the best results with smaller tumors and no ascites accumulation. The average +/-SEM is reported in fig. with at least 5 mice per treatment group.

C. *Effect of MSC1- over MSC-therapy in MOSEC model.* Once the optimal treatment regimen and cell dose that consistently lead to tumor suppression are established, then a battery of donors (at least 5) induced into *MSC1* will be evaluated for a direct comparison of MSC-therapy. Tumor growth and spread will be measured and presented as above. (Months 6-12, 120 C57Bl/6J mice)

Task 1.C *Experiments in Progress*

Group	Vehicle Control	MSCs	MSC1
1	8	-	-
2	-	8	-
3	-	-	8

Vehicle control mice will receive IP injections with HBSS (0.1mL). MSCs-are animals that will receive MSCs prepared by standard unmodified methodology, *MSC1*-animals receive MSCs primed by our methodology into a uniform phenotypes. All animals will be harvested at day 75. MOSEC mice will be treated IP with 0.1 mL MSCs, *MSC1*, or vehicle by the optimal method determined from

aim 1.1 and 1.2. Data will be presented as above. This experiment will require a total of 24 animals. Since 5 donors will be tested a total of **120 animals** will be needed.

Task 2. **Determine the anti-tumor mechanisms established by *MSC1*-treatment of MOSEC mice.** (Months 12-24):

A. *TME changes made by the MSC-based therapies.* (Months 12-24, 96 C57Bl/6J mice)

Group	Day of Animal Sacrifice	Vehicle Control	MSCs	MSC1
1	40 (early)	8	8	8
2	60 (late)	8	8	8

The MOSEC mice will be treated intraperitonealy (IP) with MSCs, *MSC1*, or vehicle on the optimal treatment day determined above. TME changes will be determined in MOSEC mice optimally treated with vehicle control, MSCs or *MSC1* as established in aim 1.1 and 1.2. Animals will be sacrificed on day 40 (early) or 60 (late) and tumor lysates will be prepared for RNA, protein, and cell analysis. Tumor extracts will be assayed for soluble inflammatory factors and immune cells. This experiment will require a total of 48 animals. Since 2 donors will be tested a total of **96 animals** will be needed.

Effect on inflammatory soluble factors in the TME TME changes will be determined in MOSEC mice optimally treated with vehicle control, MSCs, or *MSC1* as established in aim 1. Animals will be sacrificed on day 40 (early) or 60 (late) and tumor lysates will be prepared for RNA, protein, and cell analysis. Tumor extracts will be assayed for soluble inflammatory factors including TNFα, IFNγ, IL6, IL10, pro-angiogenic factors EGF, PDGF-BB, CXCL10, and other factors associated with Th1, Th2, and Th17 responses by BioPlex bead based assays as before.[Coffelt, Tomchuck et al. 2009; Waterman, Tomchuck et al. 2010] Separate commercially available kits will be used for LL37, TGFβ and PGE2 measurements. Western Blotting or IHC will be used to determine ECM proteins.[Coffelt, Tomchuck et al. 2009; Waterman, Tomchuck et al. 2010] Changes in the RNA for all of these factors and proteases (metalloproteases, MMP2, 9, 14 and uPA) important in tumor spread will be measured by qPCR. Evaluation of migration by tumor cells to complement the ECM and MMP data will be done as previously described.[Tomchuck, Zwezdaryk et al. 2008; Coffelt, Tomchuck et al. 2009]

Effect of *MSC*-therapy on immune cell recruitment to TME We will determine the relative contribution of the MSC-based therapy on TME immune cell accumulation in ovarian cancer using immunohistochemistry (IHC) and multi-color flow cytometry. Tumors from MOSEC mice treated with vehicle, MSCs, or *MSC1*, as above will be collected on day 40 and day 60. For IHC, tumor biopsy samples will be stained with antibodies to macrophages (CD68, F4/80), memory T cells (CD45RO), B cells (CD19), or neutrophils (Gr-1) as appropriate. Image analysis will be performed as previously described to quantify cell number.[Coffelt, Waterman et al. 2008; Coffelt, Marini et al. 2009; Coffelt, Tomchuck et al. 2009] For flow cytometry, single cell suspensions of collected tissues will be achieved as before.[Nesbeth, Scarlett et al. 2009; Waterman, Tomchuck et al. 2010] Analysis of immune cell markers expressed from the obtained tissue will be done by multi-color cell surface antibody staining as in those studies, or as indicated for the specific T cell subsets. Intracellular cytokine, FOXP3, RORγt, etc. antibody staining is achieved after fixation and permeabilization of the cells. Isotype controls and unstained samples will be run in parallel as standard. End point flow cytometry analysis will be performed on a BD LSRII analyzer. Cell sorting for immune cell subsets will be performed on a BD FACSAria and analyzed with CellQuest software.

Task 2.A *Experiments in Progress*

B. *Systemic immune responses affected by MSC-therapy of MOSEC mice* (Months 12-24, 144 C57Bl/6J mice)

Group	Day of Animal Sacrifice	Vehicle Control	MSCs	MSC1
1	30 (prior to MSC therapy)	8	8	8
2	60 (mid-MSC therapy)	8	8	8
3	75 (full course of tx)	8	8	8

Vehicle control mice will receive IP injections with HBSS (0.1mL). MSCs-are animals that will receive MSCs prepared by standard unmodified methodology, *MSC1*-animals receive MSCs primed by our methodology into uniform phenotypes. Host immune responses will be determined in MOSEC mice optimally treated with vehicle control, MSCs or *MSC1* as established in aim 1.1 and 1.2. Animals will be sacrificed on day 30 (before start of MSC-tx), day 60 (mid MSC-tx) or 75 (after full course of tx). Blood, spleen and draining lymph nodes will be collected at time of harvest and tested for soluble inflammatory factors (2.2a) and immune cells (2.2b,c). This experiment will require a total of 72 animals. Since 2 donors will be tested a total of **144 animals** will be needed.

Effect of *MSC*–therapy on inflammatory mediators Blood will be collected from euthanized animals by cardiac puncture and the derived serum will be tested as described above for inflammatory factors.

Effect on T cell subsets in ovarian tumors by *MSC*-therapy To complement the studies in TME, central lymphoid responses will also be evaluated. MOSEC mice will be treated as before with vehicle, MSCs, or *MSC1*. On days 40, and 60, spleen and draining lymph nodes will be harvested and the overall immune cells profile established as described above. Splenocytes and lymph node tissues will be activated with PMA-ionomycin and gene expression quantified by qPCR for FoxP3, RORγt, IL-4, IFNγ, and IL-17A to assess the expression of Th1, Th2, Th17, and Treg related genes.

Effect of *MSC*-therapy on tumor antigen-specific T cell responses To determine the effect of *MSC*-therapy on T cell responses, the tumor and regional lymph nodes of MOSEC mice treated with vehicle, MSCs, or *MSC1* as above will be collected at end of experiment. T cells will be stimulated with ConA or MOSEC tumor lysates. Cell proliferation will be determined by CFSE assays and supernatants will be assayed for IL-4, IL-17A, IL-10, and IFNγ. (Waterman, Tomchuck et al. 2010) T cell subset analysis will also be performed on permeabilized cells by flow cytometry to quantify FoxP3, RORγt, IL-4, IFNγ, and IL-17A positive cells as above.

Task 2.B *Experiments in Progress*

We have started with developing the flow cytometry and immunohistochemical protocols. We have had to test various antibodies in each assay. We are close to having these assays optimized so that it will yield answers to the anti-tumor immune mechanism supported by the optimal *MSC1* therapy of this ovarian cancer model. We have also developed an anti-TRAIL IHC protocol since we hypothesize that *MSC1* is driving increased TRAIL secretion to mediate the anti-tumor response. We have also purchased the cytokine and chemokine bead arrays to determine the soluble factors mediated by the anti-tumor *MSC1* therapy.

Development of a Diagnostic Multiplex qPCR ASSAY

In anticipation of the need to standardize the *MSC1* preparation during scale-up and clinical grade production we have developed multiplex qPCR assays with 5 genes and 4 miRNA that can predict with a high confidence interval (>99%) the anti-tumor potency of each *MSC1* preparation. During each *MSC1* preparation we extract miRNA and RNA from a working cell stock and have designed specific primers to evaluate the levels of 5 unique genes and 3 miRNAs. This methodology will soon be submitted as a patent application and thus cannot disclose all of the genes and miRNAs. We will develop this assay as a new diagnostic kit for others interested in using our improved MSC technology. One of the genes used is revealed here since it is relevant to the goal of this work: trying to understand the anti-tumor mechanism of *MSC1* therapy. We are pursuing TRAIL as a key molecule in this process.

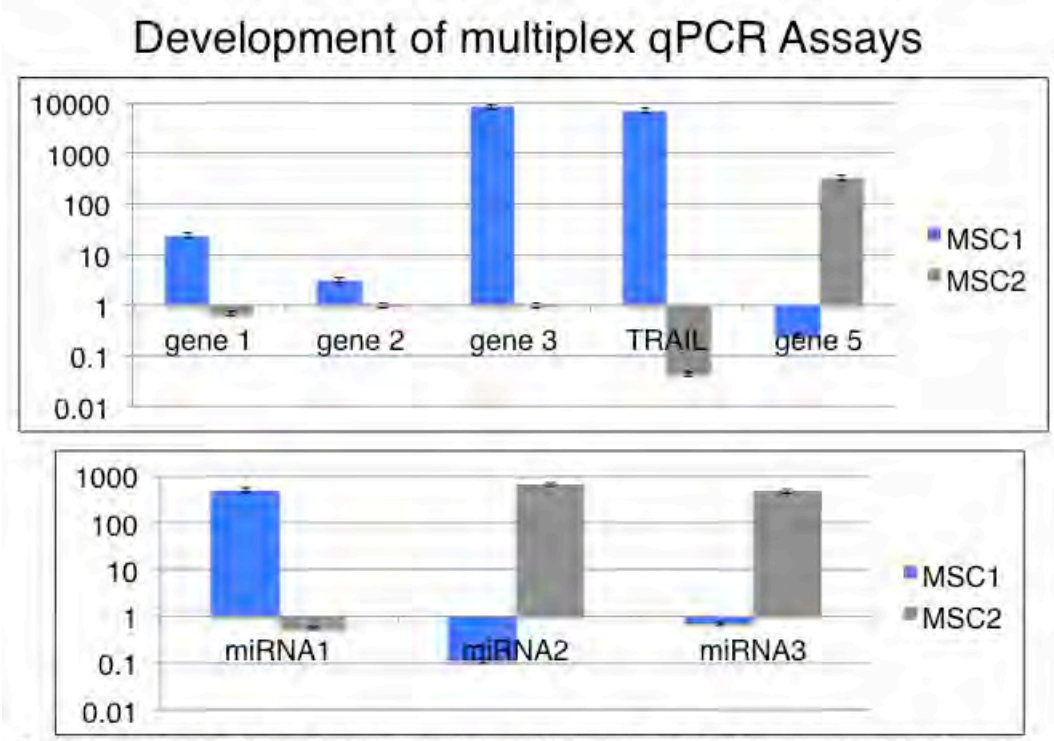

Conclusion: We developed multiplex qPCR assays that can consistently be used to assess *MSC1* identity and anti-tumor potency .

KEY RESEARCH ACCOMPLISHMENTS:

We were the first to show that:

- Human bone marrow derived mesenchymal stem/progenitor cells (MSCs) can be induced into a more homogeneous and predictable anti-tumor *MSC1* phenotype.
- We have now consistently tested the anti-tumor *MSC1* cell therapy in a relevant immune COMPETENT mouse model of ovarian cancer.
- Studies in this project have now determined the optimal cell dose, time and regimen for the anti-tumor *MSC1* cell therapy.
- Complementary efforts to develop this therapy for the clinic are underway, we have developed a diagnostic kit in anticipation of scaling up and manufacture of the *MSC1* cell therapy.
- We have submitted SBIR proposals that will help quickly translate the anti-tumor *MSC1* therapy from the lab to the clinic.

REPORTABLE OUTCOMES:

Publications:

1. Yang M, Stapor PC, Peirce SM, **Betancourt, A.M**. and Murfee, W.L. (**2012**) Rat Mesentery Exteriorization: A Model for Investigating the Cellular Dynamics Involved in Angiogenesis. J Vis Exp. 2012:e3954.
2. Ryan W. Bonvillain, Svitlana Danchuk, Deborah E. Sullivan, **Aline M. Betancourt**, Julie A. Semon, Michelle E. Eagle, Jacques P. Mayeux, Ashley N. Gregory, Guangdi Wang, Ian K. Townley, Zachary D. Borg, Daniel J. Weiss, MD, and Bruce A. Bunnell. (**2012**) A Non-Human Primate Model Of Lung Regeneration: Detergent-Mediated Decellularization And Initial Recellularization With Mesenchymal Stem Cells, In Vitro. Tissue Eng. Part A. 2012 Aug 23.
3. Ruth S. Waterman, Jenny Morgenweck, Bobby D. Nossaman, Anna E. Scandurro, Sophia A. Scandurro, and **Aline M. Betancourt**. (**2012**). Anti-Inflammatory Mesenchymal Stem Cells (MSC2) Attenuate Symptoms of Painful Diabetic Peripheral Neuropathy. Stem Cells Transl. Med. July 9. 557-565.
4. Ruth S. Waterman, Sarah L. Henkle, and **Aline M. Betancourt**. (**2012**) Mesenchymal Stem Cell 1 (MSC1)-based therapy attenuates tumor growth whereas MSC2-treatment promotes tumor growth and metastasis. PLoS ONE 7(9): e45590. doi:10.1371/journal.pone.0045590 Aug. 2012.
5. Suzanne L. Tomchuck, Sarah L. Henkle, Seth B. Coffelt, and **Aline M. Betancourt**. (**2012**) Toll-Like Receptor 3 and Suppressor of Cytokine Signaling Proteins Regulate CXCR4 and CXCR7 Expression in Bone Marrow-Derived Human Multipotent Stromal Cells. PLoS One. 2012;7(6):e39592. Epub 2012 Jun 22.
6. Zhang S, Danchuk SD, Imhof KM, Semon JA, Scruggs BA, Bonvillain RW, Strong AL, Gimble JM, **Betancourt AM**, Sullivan DE, Bunnell BA. (**2013**) Comparison of the therapeutic effects of human and mouse adipose-derived stem cells in a murine model of lipopolysaccharide-induced acute lung injury. Stem Cell Res Ther. 2013 Jan 29;4(1):13.

Book Chapters:

1. **Aline M. Betancourt** and Ruth S. Waterman (**2012**). The Role of Mesenchymal Stem Cells in the Tumor Microenvironment, Tumor Microenvironment and Myelomonocytic Cells, Subhra K. Biswas (Ed.), ISBN: 978-953-51-0439-1, InTech, Available from: http://www.intechopen.com/books/tumor-microenvironment-and-myelomonocytic-cells/the-role-of-mesenchymal-stem-cells-in-the-tumor-microenvironment
2. **Aline M. Betancourt**. New Cell-Based Therapy Paradigms: Polarization of Bone Marrow-Derived Multipotent Stromal Cells into Pro-inflammatory (MSC1) and Anti-Inflammatory (MSC2) Phenotypes. Advances in Biochemical Engineering/Biotechnology, "Mesenchymal stem cells - origin and characteristics, functions and perspectives for clinical use" M. Dominici ed, **2012**, 1-35, DOI: 10.1007/10_2012_141 Springer Publishing Co.

Presentations:

- Building Towards a Standard for MSCs: a UK-US (NIH)-Canada-led Workshop Bethesda 2013
- 6th International Symposium on Mesenchymal Stem/Progenitor Cells Texas 2013

Submitted Research Support:

PHS2012-1-1(Betancourt)	9/1/13-8/31/14
7.2 calendar	
NIH/NCI	$200,000

The First Targeted Mesenchymal Stem Cell-Based Therapy of Cancer

The overall goal of this Phase I study is to generate “proof of principle” data validating that expanded and banked clinical grade MSC1 are consistently anti-tumor in cell-based therapies of an ovarian cancer animal model.

CONCLUSION:

In this TEAL Expansion Award project we aim to:

Pre-clinically evaluate a new cell-based MSC therapy for ovarian cancer that has the potential to shift the ovarian tumor microenvironment from a pro-tumor one to a tumor eradicating one. There are over 20 ongoing or completed clinical trials that have established that mesenchymal stem cell (MSC)-based therapies are safe and effective in the treatment of many human diseases. MSCs derived from various *adult* tissues naturally track to inflamed sites and help to heal these sites by their anti-inflammatory properties. Both self (autologous) and non-self (allogeneic) MSC-based therapies are confirmed as safe and effective. As a result, many new and existing businesses are developing off-the-shelf allogeneic MSC-based products for the treatment of a wide-ranging set of human diseases including cancer. In this proposed work we will gain information and collect evidence for an improved method (phenotype induction) to prepare and deliver anti-tumor MSCs (*MSC1*) to the ovarian cancers.

Identify the molecular details behind the contributions of tumor-resident MSCs to ovarian cancer growth and spread. This approach has the potential to identify new targets for preventive and therapeutic interventions of ovarian cancer, as well as to determine the contributions of stromal components to ovarian cancer growth and spread. Therefore, by providing a clear understanding of the distinct contributions by tumor-resident MSCs and *MSC1*, these studies should lay the groundwork for cell-based therapies that inhibit tumor growth and spread.

We are well under way in our study goals. We have completed the work to date as planned and we have the personnel that we need to successfully complete this project.

REFERENCES:

(PMCID numbers follow references)

1. Coffelt SB, Ruth S. Waterman, Luisa Florez, Kerstin Höner zu Bentrup, Kevin J. Zwezdaryk, Suzanne L. Tomchuck, Heather L. LaMarca, Elizabeth S. Danka, Cindy A. Morris, and Aline B. Scandurro: **Ovarian cancers overexpress the antimicrobial protein hCAP-18 and its derivative LL-37 increases ovarian cancer cell proliferation and invasion.** *International Journal of Cancer* 2007, **in press**
2. Coffelt SB, Marini FC, Watson K, Zwezdaryk KJ, Dembinski JL, LaMarca HL, Tomchuck SL, Honer zu Bentrup K, Danka ES, Henkle SL, Scandurro AB: **The pro-inflammatory peptide LL-37 promotes ovarian tumor progression through recruitment of multipotent mesenchymal stromal cells.** *Proc Natl Acad Sci U S A* 2009, **106:**3806-3811.2656161
3. Coffelt SB, Tomchuck SL, Zwezdaryk KJ, Danka ES, Scandurro AB: **Leucine leucine-37 uses formyl peptide receptor-like 1 to activate signal transduction pathways, stimulate oncogenic gene expression, and enhance the invasiveness of ovarian cancer cells.** *Mol Cancer Res* 2009, **7:**907-915.2755540
4. Coffelt SB, Waterman RS, Florez L, Honer zu Bentrup K, Zwezdaryk KJ, Tomchuck SL, LaMarca HL, Danka ES, Morris CA, Scandurro AB: **Ovarian cancers overexpress the antimicrobial protein hCAP-18 and its derivative LL-37 increases ovarian cancer cell proliferation and invasion.** *Int J Cancer* 2008, **122:**1030-1039
5. Tomchuck SL, Zwezdaryk KJ, Coffelt SB, Waterman RS, Danka ES, Scandurro AB: **Toll-like receptors on human mesenchymal stem cells drive their migration and immunomodulating responses.** *Stem Cells* 2008, **26:**99-107
6. Waterman RS, Tomchuck SL, Henkle SL, Betancourt AM: **A new mesenchymal stem cell (MSC) paradigm: polarization into a pro-inflammatory MSC1 or an Immunosuppressive MSC2 phenotype.** *PLoS One* 2010, **5:**e10088.2859930
7. Singh P, Williams DJ: **Cell therapies: realizing the potential of this new dimension to medical therapeutics.** *J Tissue Eng Regen Med* 2008, **2:**307-319
8. Salem HK, Thiemermann C: **Mesenchymal stromal cells: current understanding and clinical status.** *Stem Cells*, **28:**585-596.2962904

APPENDICES: Attach all appendices that contain information that supplements, clarifies or supports the text. Examples include original copies of journal articles, reprints of manuscripts and abstracts, a curriculum vitae, patent applications, study questionnaires, and surveys, etc.

Personnel that worked on the study include graduate student Derek Dashti and post-doctoral fellow Dr. Shuguang Wang, PhD

1 reprint follows- PLoS ONE 11 pages

Mesenchymal Stem Cell 1 (*MSC1*)-Based Therapy Attenuates Tumor Growth Whereas *MSC2*-Treatment Promotes Tumor Growth and Metastasis

Ruth S. Waterman[1], Sarah L. Henkle[2], Aline M. Betancourt[2,3]*

1 Department of Anesthesiology, Ochsner Clinic Foundation, New Orleans, Louisiana, United States of America, **2** Tulane Center for Stem Cell Research and Regenerative Medicine, Tulane University School of Medicine, New Orleans, Louisiana, United States of America, **3** Department of Medicine, Tulane University School of Medicine, New Orleans, Louisiana, United States of America

Abstract

Background: Currently, there are many promising clinical trials using mesenchymal stem cells (MSCs) in cell-based therapies of numerous diseases. Increasingly, however, there is a concern over the use of MSCs because they home to tumors and can support tumor growth and metastasis. For instance, we established that MSCs in the ovarian tumor microenvironment promoted tumor growth and favored angiogenesis. In parallel studies, we also developed a new approach to induce the conventional mixed pool of MSCs into two uniform but distinct phenotypes we termed *MSC1* and *MSC2*.

Methodology/Principal Findings: Here we tested the *in vitro* and *in vivo* stability of *MSC1* and *MSC2* phenotypes as well as their effects on tumor growth and spread. *In vitro* co-culture of *MSC1* with various cancer cells diminished growth in colony forming units and tumor spheroid assays, while conventional MSCs or *MSC2* co-culture had the opposite effect in these assays. Co-culture of *MSC1* and cancer cells also distinctly affected their migration and invasion potential when compared to MSCs or *MSC2* treated samples. The expression of bioactive molecules also differed dramatically among these samples. *MSC1*-based treatment of established tumors in an immune competent model attenuated tumor growth and metastasis in contrast to MSCs- and *MSC2*-treated animals in which tumor growth and spread was increased. Also, in contrast to these groups, *MSC1*-therapy led to less ascites accumulation, increased CD45+leukocytes, decreased collagen deposition, and mast cell degranulation.

Conclusion/Significance: These observations indicate that the *MSC1* and *MSC2* phenotypes may be convenient tools for the discovery of critical components of the tumor stroma. The continued investigation of these cells may help ensure that cell based-therapy is used safely and effectively in human disease.

Citation: Waterman RS, Henkle SL, Betancourt AM (2012) Mesenchymal Stem Cell 1 (*MSC1*)-Based Therapy Attenuates Tumor Growth Whereas *MSC2*-Treatment Promotes Tumor Growth and Metastasis. PLoS ONE 7(9): e45590. doi:10.1371/journal.pone.0045590

Editor: Paolo Fiorina, Children's Hospital Boston/Harvard Medical School, United States of America

Received April 24, 2012; **Accepted** August 23, 2012; **Published** September 20, 2012

Copyright: © 2012 Waterman et al. This is an open-access article distributed under the terms of the Creative Commons Attribution License, which permits unrestricted use, distribution, and reproduction in any medium, provided the original author and source are credited.

Funding: Funding was provided to AMB by the National Institutes of Health 1P20RR20152-01, Department of Defense OC073102 Concept Award and research support from the Tulane Cancer Center and the Center for Stem Cell Research and Regenerative Medicine. Funding was provided to RSW by the Foundation for Anesthesiology Education and Research (FAER). The funders had no role in study design, data collection and analysis, decision to publish, or preparation of the manuscript. No additional external funding was received for this study.

Competing Interests: Aline M. Betancourt is the inventor of the patent-pending "Mesenchymal Stem Cells and Related Therapies" (MSC1 and MSC2 methodology) US 61/391,749. Aline M. Betancourt is Founder and Chief Financial Officer for wibi+works, LLC without any salary, benefit or income. As inventor of the patent stated above there are no interests, products, benefits, compensations, or salary. Ruth S. Waterman is the Chief Executive Officer for wibi+works, LLC without any benefit, salary, or income. There are no further patents, products in development or marketed products to declare. This does not alter the authors' adherence to all the PLOS ONE policies on sharing data and materials.

* E-mail: alibscan@tulane.edu

Introduction

Mesenchymal stem cells (MSCs, more accurately termed multipotent mesenchymal stromal cells) are increasingly being used in cell-based therapies of diseases ranging widely from graft-versus-host to joint and cartilage disorders [1,2]. There are many features that make these cells attractive and practical for use in human therapy. First, MSCs are easily obtained from various adult-derived tissues, quickly expanded, and stored *ex vivo* without significant impact to their capabilities. Second, once reintroduced, MSCs preferentially home to sites of injury or inflammation and support healing and repair mostly through the local secretion of bioactive factors and modulation of immune cells. Third, MSCs from non-self (allogeneic) or self (autologous) donors can be used safely since they do not elicit harmful immune responses within the recipient host. Lastly, pre-clinical studies have demonstrated efficacy with MSCs genetically engineered to carry various therapeutics that reached their target with significant treatment benefit even in the xenogeneic setting (human cells to mouse host) (recently reviewed [3–5]).

Despite these promising features, there is a growing concern over the clinical use of MSCs since they are also known to home to tumors and once resident in the tumor microenvironment (TME) to support tumor growth and spread [4–8]. Conversely, other studies have reported that MSCs found in the TME diminish tumor growth, which has further generated some controversy in

this field (reviewed in [4,5]). Other noted concerns in the clinical use of MSCs, is the fact that we still do not have a general consensus of what defines them, and furthermore although one of their most profound clinical effects upon intravenous administration is the modulation of host immune responses, we do not yet truly understand all of their consequences upon introduction into the host [1,9,10]. Either way, as a result of the established clinical properties of MSC and their added propensity for the TME, modified MSCs that can act as "Trojan horses" and deliver anti-cancer therapeutics into the tumor stroma are being evaluated as a promising new targeted cell-based therapy for cancer [4,5].

MSCs targeted to cancers are expected to contribute many soluble factors such as mitogens, extracellular matrix (ECM) proteins, angiogenic, and inflammatory factors, as well as exosomes or microvescicles, once resident in the TME [3–5]. MSCs are also expected to affect tumor-associated leukocytes either directly by cell-cell contact or indirectly by the secretion of trophic factors [3–5]. MSCs are known to affect the proliferation and differentiation of dendritic cells, monocytes/macrophages, B and T cells, NK cells, and even mast cells [3–5]. Many reasons have been advanced to explain the contradictory MSC role in cancer including but not limited to the heterogeneity of MSC preparations, the age or health of the MSC donor, and the experimental model or condition [3–5].

Our group established that MSCs in the ovarian tumor microenvironment promoted tumor growth and favored angiogenesis [7,11,12]. We also developed new methodology to induce the conventional mixed pool of MSCs into two uniform but distinct phenotypes, *MSC1* and *MSC2* [13]. These phenotypes were recently and successfully tested in the therapy of a mouse model of painful diabetic peripheral neuropathy [14]. This study also demonstrates the stability of these newly defined phenotypes in cell-based treatment of an immune competent disease model. We initially based their classification on several parallel observations reported within the monocyte literature. Like MSCs, heterogeneous bone marrow-derived monocytes respond to stress or "danger" inflammatory signals and home to tissue injury. Monocyte polarization into the classically activated pro-inflammatory macrophages (M1) occurs early on in tissue repair, whereas monocyte polarization into alternatively activated macrophages (M2) follows later to help in tissue injury resolution [15,16]. Although, this is a very simplified view of what occurs in the complex process of wound healing and repair, it provides a convenient paradigm to begin to dissect critical components within this complex biological process [17–19].

In this study, we similarly took advantage of this convenient paradigm in MSCs as a way to potentially resolve some of the controversy surrounding the complex role of MSCs in cancer. Indeed, *MSC1* and *MSC2* were found to have divergent effects on cancer growth and metastasis by *in vitro* and *in vivo* methods. In our experiments, *MSC1* primarily had an anti-tumor effect, whereas *MSC2* promoted tumor growth and metastases. We suggest that further investigation of these cells may provide some guidance in designing safer and more efficacious MSC-based therapies.

Results

MSC1 do not Support *in vitro* Tumor Cell Growth Whereas *MSC2* Favor Tumor Cell Growth

To further extend our studies on the role of MSCs and ovarian tumors we initially investigated the effect of the recently described *MSC1* and *MSC2* phenotypes on various cancer cell lines [7,12,13,20]. The effect of MSCs, *MSC1,* or *MSC2* on the growth of various cancer cell lines was determined by traditional 2D-colony forming units (CFU) and 3D- tumor spheroid formation assays (Figure 1). Please note that the ratio of cancer cells to MSCs used was 10 to 1 respectively. As expected co-culture with MSCs led to more breast (MDA-MB-231), pancreas (PANC-1) and ovarian (OVCAR, SKOV3, MOSEC) cancer cell colonies and larger tumor spheroids compared to untreated controls (Fig. 2A, B Figures S1 and S2, and data not shown). By contrast, *MSC1*-cancer co-culture consistently led to fewer colonies and much smaller tumor spheroids. Each cancer cell line exhibited their own unique morphology when grown in the CFU and tumor spheroids. It is expected that at a 10:1 cancer cell to MSC ratio the body of the colonies and spheroids are primarily composed of the cancer cells. This is supported by the observed unique morphologies recorded for each cancer cell line treated with the MSCs. *MSC2* co-culture resulted in the greatest number of CFUs and largest spheroids. We noted that typically the MSCs and *MSC2* co-cultures led to bigger and more diffuse colonies and spheroids whereas the *MSC1* resulted in smaller, tighter, and more compact CFUs and tumor spheroids. CellTracker green labeled MSCs and *MSC2* in the tumor spheroid assays mostly distributed throughout the spheroids (Figure S2). These *in vitro* assays' results suggest that MSCs and *MSC2* support tumor cell growth whereas *MSC1* seem to diminish tumor cell growth.

We also measured the cytokines, chemokines, and other bioactive factors secreted into the medium by the MSC-cancer cell co-cultures as before (Table 1, [13,20]). In these experiments we have no means of distinguishing which cell; MSC or cancer, is contributing the bioactive factors, we can simply detect the net effect of the co-culture conditions used here. SKOV3 ovarian cancer cells were plated on 24-well plates until they reached 50–70% confluence. *MSC1*, *MSC2*, (25,000 cells/insert) or medium control were then added into 0.4 μM (no cancer cell-MSC contact) or 8 μM transwell inserts and the co-cultures were allowed another 72 hr prior to collecting the conditioned medium and testing by BioPlex assay. *MSC1*-treated samples elaborated higher levels of pro-inflammatory factors including IL17, IL3, MIG, MIP1β and GM-CSF whereas *MSC2*-treated samples had marked increases in ILRA, IL10, CXCL1, CCL5 and CXCL10 (Table 1). Interestingly, TNF-related apoptosis-inducing ligand (TRAIL) expression was dramatically induced in *MSC1*-treated co-cultures when compared to *MSC2*-treated ones. By contrast, the expression of GM-CSF, LIF, and TRAIL was attenuated in *MSC2*-treated samples when compared to *MSC1*-treated ones. We observed similar trends when we sampled the biofactor secretion from the 3D tumor spheroid co-cultures (data not shown).

Migration and Invasion of Cancer Cells Following MSC Phenotype Co-culture

We next examined the effect on the migration and invasion capabilities of these cancer cells following co-culture with the MSCs, *MSC1,* and *MSC2*. Similar to the previous report that conventionally derived MSCs promote MDA-MB-231 breast cancer cell migration and invasion [8], we also found that migration and invasion was promoted by MSCs and *MSC2* but not by *MSC1* (Figure 2). We observed about a two-fold increase in both migration and invasion assays by MSCs and *MSC2* co-culture (Figure 2A and B, respectively). In our experiments, all MSCs were added at a 10:1 ratio of cancer cells to MSC as before. We tested the effect of co-culture of the cells plated in traditional 2D dishes 72 hr prior to placing the dissociated cells within the transwell inserts. We also tested the effect of the MSCs on the 3D tumor spheroids grown cancer cells after subsequent dissociation and loading in transwell inserts for these assays (Figure 2A and B). We

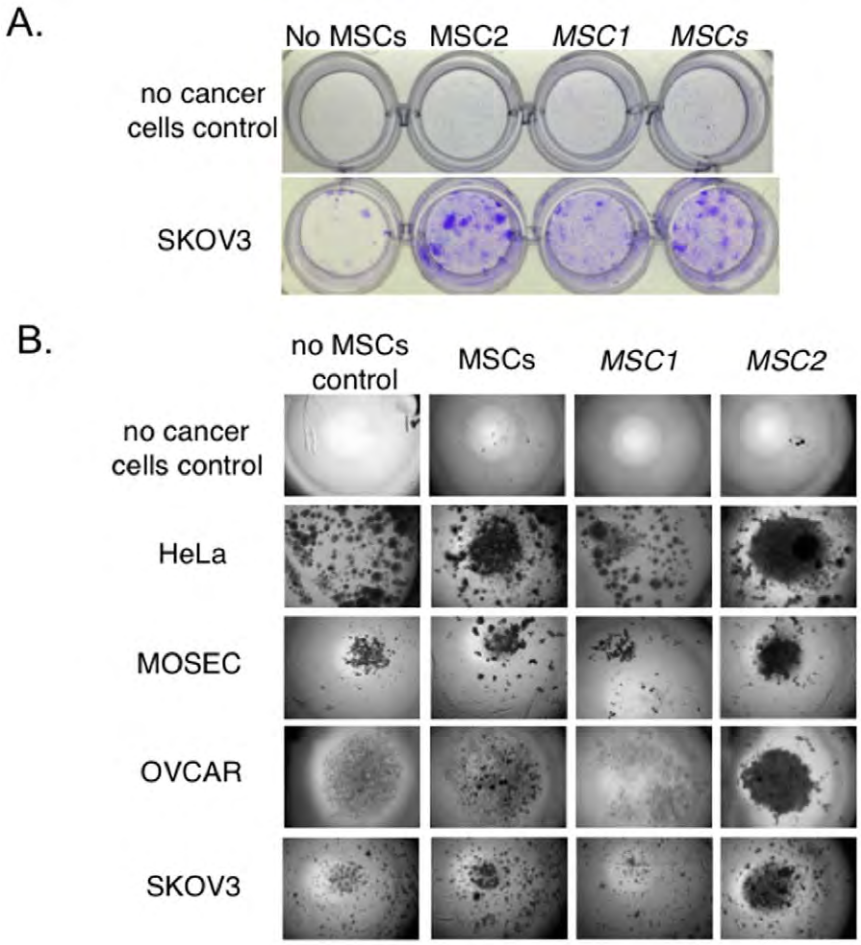

Figure 1. *MSC1* do not support tumor cell growth whereas *MSC2* favor tumor cell growth. A. Representative micrographs from colony forming units (CFU) assays performed by culturing human tumor cells (200 cells/well) mixed with MSCs, *MSC1*, or *MSC2* (2 cells/well) at a ratio of 10 cancer cells per 1 MSC and plated in 24-well plates in growth medium supplemented with 10% FBS as indicated in figure. Cultures were grown for 14 days at 37°C in a humidified atmosphere of 5% carbon dioxide balance air. Growth medium was changed every 3–4 days. Colonies were visualized by staining with a crystal violet solution (0.5% crystal violet/10% ethanol). The resulting colonies were enumerated by the colony counting macro in ImageJ software, SKOV3- ovarian adenocarcinoma cell lines. Colony counts are given below the micrographs. Data are representative of at least three independent experiments with at least four MSC donors. **B.** Representative micrograph of tumor spheroids formed by culturing tumor cells (200 cells/well) mixed without any other cells (–) or with MSCs, *MSC1*, or *MSC2* (20 cells/well) at a ratio of 10 cancer cells per 1 MSC and plated over 1.5% agarose in 96-well plates in growth medium supplemented with 10% FBS as indicated in figure. Cultures were grown for 14 days at 37°C in a humidified atmosphere of 5% carbon dioxide balance air. Growth medium was changed every 3–4 days. Micrographs shown represent 20Xmagnified field of the 96-well plate. Cancer cell lines used are: HeLa-human cervical adenocarcinoma, OVCAR-human ovarian adenocarcinoma, SKOV3-human ovarian adenocarcinoma, and MOSEC-murine ovarian surface epithelium carcinoma cells. Data are representative of at least three independent experiments with at least four MSC donors.
doi:10.1371/journal.pone.0045590.g001

recorded similar effects by the MSCs on the invasion and migration of the cancer cells regardless of culturing conditions.

Additionally, the effect of the MSCs, *MSC1*, and *MSC2* in these assays does not appear to correlate with their expression of matrix metalloproteinases (MMPs, Figure 2C and D). We consistently measured increased expression of several *mmp*s following MSCs induction into the *MSC1* or *MSC2* phenotypes (Figure 2C). We also observed elevated secretion of activated MMP2 (MMP2*) into the condition medium of co-cultures of *MSC1* and *MSC2* with SKOV3 when compared with medium from cultures with MSCs or SKOV3 alone (Figure 2D). Although, these levels were slightly lower than those of the MSCs samples without cancer cell co-cultures (Figure 2D). These results indicate that the distinct MSC-mediated effects on cancer migration and invasion are more complex and perhaps not directly mediated by MMP2* in agreement with the studies of the report described earlier [8].

MSC1 Attenuate Tumor Growth Whereas *MSC2* Promote Tumor Growth and Metastasis

The anti-tumor *MSC1* and the pro-tumor *MSC2 in vitro* effects were further supported in pilot studies with human ovarian cancer xenograft animal models treated with the MSC-based therapies as previously established ([7] and data not shown). We subsequently used the immune *competent* MOSEC model to verify these MSC-tumor effects (Figure 3, [21]). The tumors were established in the mice with 1×10^7 MOSEC (ID8) cells. After approximately 4 weeks a single dose of CellTracker fluorescently labeled human MSCs, *MSC1*, or *MSC2* (1×10^6/per mouse) were injected IP. The small amount of remaining MSCs preparations within the syringes were again plated and observed for contamination and subsequent growth properties. No change was noted among these spent MSC preparations in growth properties even after 2-weeks of culture.

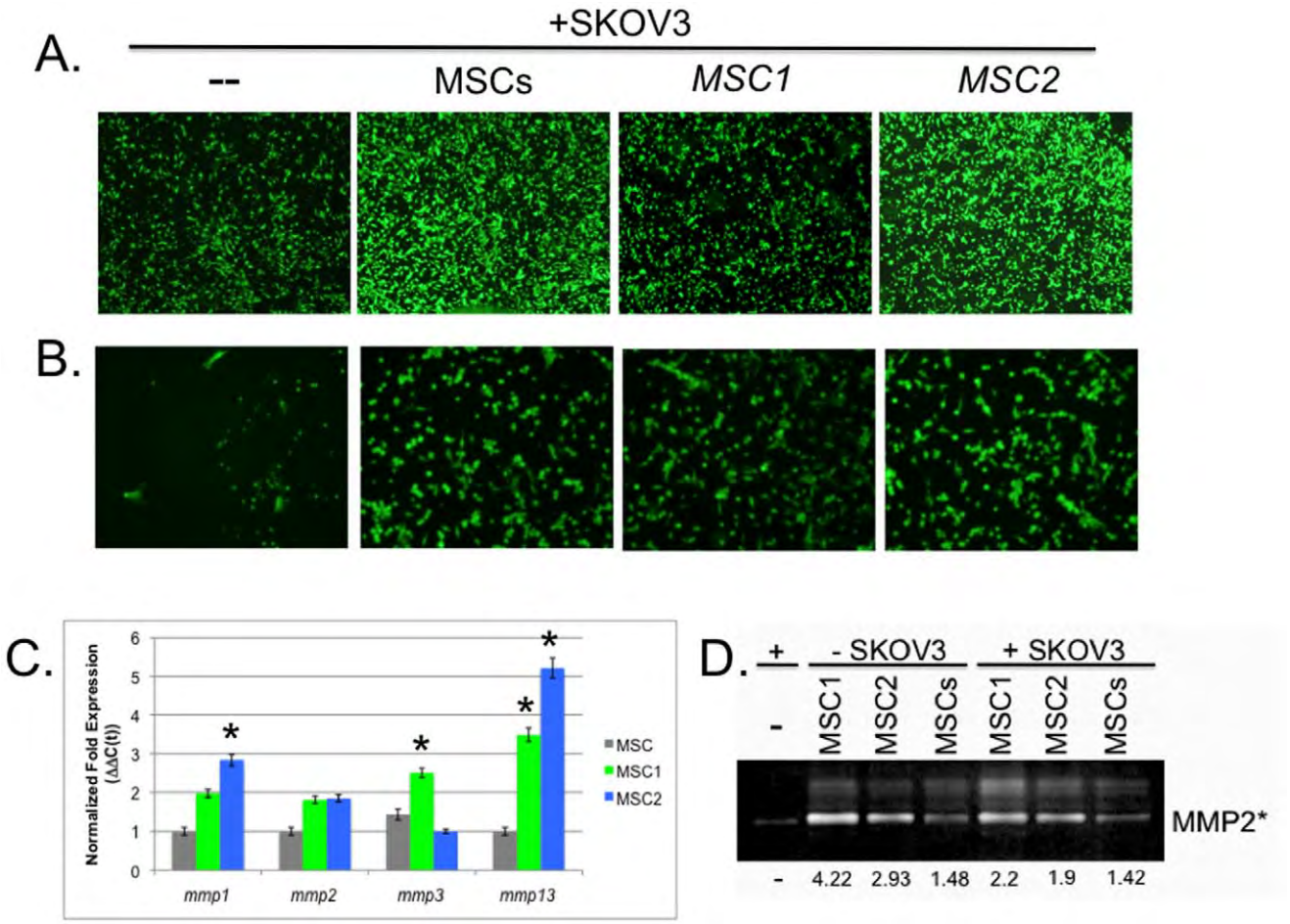

Figure 2. Migration and Invasion of Cancer Cells following MSC phenotype co-culture. Transwell migration and matrigel invasion assays were performed with 3 μM Falcon fluoroblok transwell inserts as described previously [12,20,45]. MSCs were added at a 10:1 ratio of SKOV3 to MSC. These were co-cultured on traditional 2D dishes 72 hr prior to placing the dissociated cells within the transwell inserts. Representative micrographs of **A.** transwell migrating and **B.** matrigel invading cells were visualized and obtained on an inverted fluorescence microscope (A. 100X and B. 200X, Olympus, MetaMorph analysis software). Data are representative of duplicates in at least three independent experiments**. C.** Representative bar graph of quantitative real-time PCR (qPCR) assays carried out as previously described [39]. Gene expression of *mmps* among the MSC samples is expressed by the normalized cumulative threshold method (ΔΔC(t)). *$P<0.05$ versus the normalized values for MSC. Statistically significant differences were not measured among the other samples. Samples were run in triplicate for at least four different MSC donors. **D.** Representative micrograph following gelatin zymography of the condition medium from MSC-SKOV3 co-cultures (1:10) or SKOV3 and MSC samples cultured alone as indicated for 72 hr. Bands are of pro-MMP2 (72 kDa) and active MMP2* (62 kDa). The numbers below micrograph are the fold changes relative to SKOV3 alone sample obtained following densitometric analysis (ImageJ). Data are representative of at least three independent experiments.
doi:10.1371/journal.pone.0045590.g002

Following 24 hr after the MSC-based treatments, one animal was sacrificed per treatment group to measure MSC engraftment to the primary tumor. All MSC-treated samples had similar detectable pre-labeled fluorescence MSCs within the tumor tissue trending towards more *MSC1* and *MSC2* measured than MSCs with approximately 15–25 cells versus 10–15 counted per 200X field after 24 hr of MSC-treatment (data not shown). Based on the literature and our previous experiments, MSC-based therapy of the tumor typically results in very little engraftment (<0.5%) or local proliferation of MSCs at the tumor site [10,14]. Tumor growth was measured at weekly intervals until day of mouse sacrifice (Day 65). At harvest, the ascites accumulated in the tumor bearing mice was collected. The tumors and metastases were measured and processed for flow cytometry and IHC analyses [7].

The collected ascites samples were spun down on cytospin slides and stained with Diff Quick (Figure 3B). Notably, very little (<0.5 mL/mice) to no ascites accumulated in *MSC1*-treated animals compared with MSCs- (1.25 mL/mice) and *MSC2*-treated (>5 mL/mice) animals (Figure 3C). Furthermore, *MSC2*-treated animals had the most tumor cell aggregates within the ascites followed by the MSC-treated samples, with few tumor aggregates found in *MSC1*-treated sample ascites (Figure 3B). In parallel, the tumor size and weights were biggest in *MSC2*-treated (~1500 mm^3 and 375 mg) animals followed by MSCs-treated animals (~1000 mm^3 and 283 mg) and *MSC1*-treated animals (~500 mm^3 and 167 mg, Figure 3A and C). Metastasis was found only in MSCs- and *MSC2*-treated mice.

Tumor-associated Leukocytes Differ among the MSC-treated Groups

Flow cytometry and IHC analyses of harvested tumors demonstrated some interesting differences dependent upon the MSC-treatments (Figure 4). Based on both CD45+ flow cytometry and IHC analyses *MSC1*-treated groups appeared to have the

Table 1. Ovarian cancer cells co-cultured with *MSC1* differ from *MSC2* co-cultures in their secretion of bioactive factors.

Bioactive Factor	Contact dependent effect	*MSC1*	*MSC2*
IL1RA	–	↓	↑↑
IL3	–	↑↑	↓
IL10	+	–	↑
IL12p40	–	↓	↑
IL17	+	↑↑	↑
CXCL1 (Groα)	–	↓	↑↑
CXCL10 (IP10)	+	↓	↑↑
CCL5 (RANTES)	+	−/↓	↑↑
MIG	+	↑	–
MIP1β	+	↑	↑↑
GM-CSF	+	↑↑	↓
HGF	+	↓	–
LIF	–	↑↑	↓
TRAIL	+	↑↑	↓

SKOV3 ovarian cancer cells were plated on 24-well plates until they reached 50–70% confluence. *MSC1*, *MSC2*, (25,000 cells/insert) or medium control were then added into 0.4 μM (no cell-cell contact) or 8 μM transwell inserts and the co-cultures were allowed another 72 hr prior to collecting the conditioned medium and testing by Bio-Plex Cytokine Assays following the manufacturer's instructions (Human Group I & II; Bio-Rad, Hercules, CA). Arrows represent relative normalized changes compared with the SKOV3 alone control. Biofactor levels that were different between the MSCs grown in 0.4 μM (no cell-cell contact) versus 8 μM transwell inserts are represented by "+." Those biofactor levels that were similar in both sample groups are represented by "−." Data are representative of triplicate measurements with 4 MSC donors in at least 4 independent experiments.

doi:10.1371/journal.pone.0045590.t001

greatest recruitment of leukocytes to the TME compared to the other treatment groups (Figure 4A and B). *MSC2*-treated groups also had an increased number of tumor-associated CD45+leukocytes compared to MSC-treated groups. Representative micrographs of the ImageJ threshold analysis with CD45+cells colorized red demonstrate these differences (Figure 4A). Additionally, *MSC1*-treated groups had elevated levels of F4/80+ leukocytes (likely macrophages) compared to MSCs- and *MSC2*-treated groups as determined by flow cytometry (Figure 4C). The MSCs-treated groups had the most tumor-associated neutrophils (~35%) whereas *MSC1*-treated groups had more monocytes (~40%) and *MSC2*-treated groups had close to equivalent numbers of neutrophils, monocytes and lymphocytes (~20%/each) based on differential flow cytometry analyses with specific antibodies to CD3, CD4, CD8, CD11b, CD45R, Ly-6G (Gr-1), and NKG2D (CD314) (http://phenome.jax.org/db/q?rtn=projects/docstatic&doc=Jaxpheno6/Jaxpheno6_Protocol).

Next, we used a proteoglycan-specific stain (safranin O-fast green) to help visualize the mast cells (MCs) found within the MSC-treated tumor sections (Figure 5). MCs are immune cells that are increasingly implicated in tumor growth, spread, and aggressiveness [22]. The metastatic potential of tumors is affected by the composition of the tumor associated extracellular matrix (ECM). MCs are known to promote ECM protein deposition and are associated with various human ECM disorders [23,24]. Lastly, MCs are also known to interact with MSCs [3,25]. Although we did not observe obvious differences in the number of safranin O positive mast cells in each of the MSC-treated groups, there appeared to be differences in the stained granules within the MCs among them. Specifically, while MSC- and *MSC2*-treated tumor sections appeared to contain mostly safranin O-positive granule laden MCs, *MSC1*-treated tumor sections contained mostly MCs that appeared degranulated (insets of Figure 5). We also noted that the MCs were distributed mostly throughout the stromal fibrovascular compartments of all tumors where they may also be acting to affect the ECM (Figures S3 and S4). These results indicate that the anti-tumor *MSC1*-effects and the pro-tumor *MSC2*-effects may be mediated by differences in their ability to distinctly affect various tumor-associated leukocytes as well as directly or indirectly affect the ECM content of the tumor microenvironment.

Discussion

The novel finding of this study is that mesenchymal stem cells (multipotent stromal cells, MSCs) induced into the *MSC1* phenotype attenuate cancer cell growth while MSCs induced into the *MSC2* phenotype mostly mimic conventional MSCs in promoting cancer cell growth and spread. Additionally, that once the *MSC1* and *MSC2* phenotypes are induced and reintroduced they appear to lead to distinct tumor effects. In another complementary study, we similarly tested for the stability of the induced phenotypes and their distinct therapeutic effects in a murine model of pain [14].

Recently, a shadow has been cast over the successful and increasing use of MSC-based therapies in many diseases, by the growing controversy of whether the MSCs used in the treatment might promote tumor growth as some preclinical studies, including ours, suggest [7]. By contrast, others have argued that MSCs attenuate tumor growth and spread. However, most agree that as a result of the propensity of MSCs to home to tumors, these cells used in cell therapies of cancer provide ideal cancer drug delivery vehicles [4–6,26]. In this study, we present evidence that might shed some light over these controversies and that may provide some guidance in the design of safer MSC-based therapies.

We extended our work on MSCs and ovarian cancer, as well as our study describing a new approach for the induction of MSCs into a pro-inflammatory *MSC1* and an immunosuppressive *MSC2* phenotype. Accordingly, we chose to focus our investigation on the distinct effect that *MSC1* and *MSC2* might have on tumor growth and spread compared to the established one with conventionally prepared MSCs [7,13]. Our initial *in vitro* experiments demonstrated that *MSC1* co-culture with various cancer cells diminished their capacity to form colonies in contrast to growth promoting MSC- or *MSC2*-co-cultures (Figure 1 and Figures S1 and S2). This effect remained constant even when tested by 3D tumor spheroid models. In this study we only tested cancer cells derived from solid organ tumors and not from leukemia or other blood-related malignancies. We also used MSC to cancer cell ratios of 1:10 throughout the study to more closely resemble the proportions that might be achieved in the clinic with MSC-based therapies and different to the 1:1 ratios used by other MSC and cancer studies (e.g. [8,27–29]).

MSCs targeted to cancers are expected to contribute many bioactive factors once resident in the TME, such as mitogens, extracellular matrix (ECM) proteins, angiogenic, and inflammatory factors, as well as exosomes or microvescicles. MSCs are also expected to affect tumor-associated leukocytes either directly by cell-cell contact or indirectly by these secreted factors [3]. Most of these parameters were measured in this study. We previously reported that there were differences among several of these

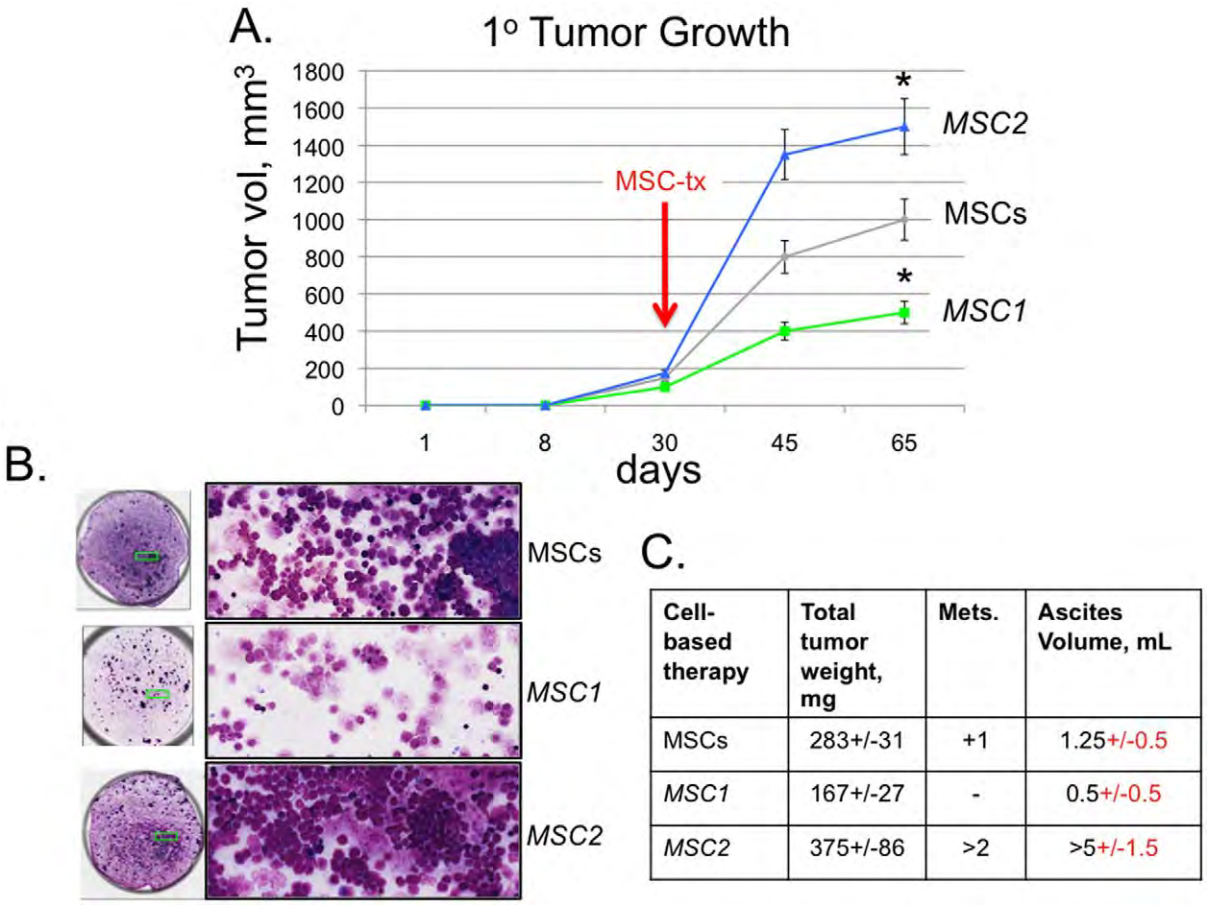

Cell-based therapy	Total tumor weight, mg	Mets.	Ascites Volume, mL
MSCs	283+/-31	+1	1.25+/-0.5
MSC1	167+/-27	-	0.5+/-0.5
MSC2	375+/-86	>2	>5+/-1.5

Figure 3. *MSC1* do not support tumor growth whereas *MSC2* favor tumor growth and metastasis. The established syngeneic mouse model for epithelial ovarian cancer used is based upon a spontaneously transformed mouse ovarian surface epithelial cell (MOSEC) line ID8 that has been previously described [21]. At approximately 4 weeks a single dose of human MSCs (MSCs), *MSC1*, or *MSC2* (1×10^6/per mouse) were injected intraperitonealy (IP) as indicated by red arrow. **A.** Tumor growth was measured at weekly intervals until day of mouse sacrifice (Day 65). Harvested tumors and metastasis were weighed, counted and processed for flow cytometry and immunohistochemical analysis (IHC). *$P<0.05$ versus the MSCs-treated tumors. **B.** Accumulated ascites was collected, measured, and a sample was spun on cytospin slides and stained by DiffQuick cytology stain by standard methods. Left circles are representative micrographs of cytospin slides (20X) with enlarged areas to the right marked by green box (100X). **C.** Table of average +/−SEM results among the different MSC-treatment groups. Data are representative of three independent experiments with at least 6 mice per treatment group.
doi:10.1371/journal.pone.0045590.g003

secreted bioactive factors following the induction of MSCs into *MSC1* and *MSC2* [13]. Co-cultures of these MSC phenotypes with the cancer cells also reflected distinct effects on the secreted factors as summarized on Table 1. Both contact-dependent and independent effects were observed. Increases measured in the levels of CCL5 (RANTES) secreted by the pro-tumor *MSC2* groups are in agreement with previous reports [8,13]. By contrast, *MSC1* treatment groups had elevated levels of IL17, GM-CSF, and TRAIL that would suggest an overall inflammatory and pro-apoptotic effect by these cells. *MSC2* treatment groups also had elevated levels of secreted IL1RA, IL10 and most chemokines tested, which suggests a net tumor supportive immunosuppressive effect by this treatment group [27]. However, it is important to recognize that the expression of bioactive factors is by necessity a dynamic process, quickly changing at any given time and place and probably confined to communication across short intercellular distances. We are also not able to distinguish the source be it MSC or cancer cell of the factors elaborated in our established co-culture experimental conditions. Furthermore, what we are able to measure with the current technology is one snapshot of time and thus it must be accordingly weighed and validated with other supportive experiments prior to drawing too many conclusions.

To this end, transwell migration and matrigel invasion capabilities were also studied (Figure 2). However, though we measured fewer migrating and invading cells for the *MSC1* sample groups compared to the other MSC sample groups, we could not attribute this difference to decreased expression of activated MMP2. Additionally, we have not been able to detect significant levels of either the zymogen or active forms of MMP9 in MSC phenotype *in vitro* cultures or co-cultures with cancer cells. These results are intriguing given the documented importance of MMP2 and 9 in tumor spread and invasion [30]. Further studies are needed to investigate this complex tumor process and how the MSCs might affect it.

Following these *in vitro* experiments, we next investigated the effects of the MSC-based therapies in an immune competent mouse model of ovarian cancer that has been useful in similar studies [21,31,32]. Since the most prevalent effect of MSC-based therapy reported in human clinical trials appears to be immune modulation, and the profile of bioactive factors primarily expressed by MSCs are immune modulatory, we thought it

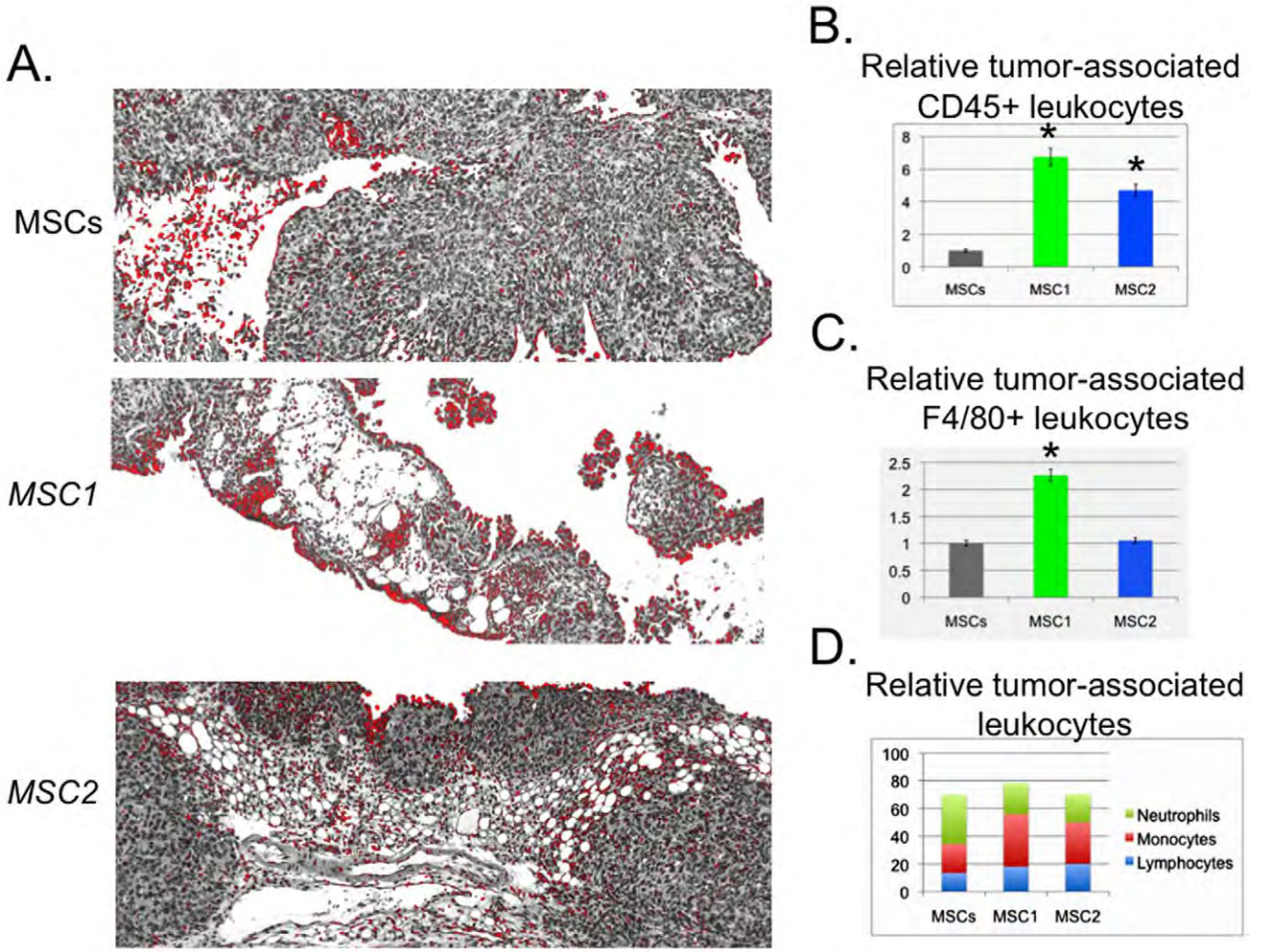

Figure 4. Tumor-associated leukocytes differ among the MSC-treated groups. MOSEC tumors were established in C57BL/6 mice for 4 weeks. MSCs, *MSC1*, or *MSC2* (1×10^6 in 0.5 mL HBSS) were infused IP and the mice were harvested after 65 days. Tumors were excised, fixed, and cut into 5 μM sections and processed for antibody staining by standard methods or single cell suspensions were made from the tumors and processed for flow cytometry analysis [7]. Data are representative of three independent experiments with at least 6 mice per treatment group. **A.** Representative micrographs of the tumor sections processed by IHC, stained with DAB, and then recorded with the Aperio ScanScope (40X, Aperio, Vista, CA). Shown is the subsequent ImageJ threshold analysis with CD45+cells colorized red. **B.** Bar graph depicting the results from the CD45+ flow cytometry analyses of the tumors relative to the MSC-treated tumors. *$P<0.05$ versus the MSCs-treated tumors. Statistically significant differences were not measured between *MSC1*- and *MSC2*-treated tumor samples. **C.** Bar graph depicting the results from the F4/80+ flow cytometry analyses of the tumors relative to the MSC-treated tumors. *$P<0.05$ versus the MSCs-treated tumors. Statistically significant differences were not measured between MSCs- and *MSC2*-treated tumor samples. **D.** Bar graph depicting the results from flow cytometry analyses to identify neutrophil, monocyte, and lymphocyte populations among the tumor samples as described in Materials and Methods. Flow cytometry data are representative of at least duplicate samples from at least three independent experiments.
doi:10.1371/journal.pone.0045590.g004

important to use immune *competent* models [2,33]. Previous studies with human MSCs introduced into allogeneic or xenogeneic hosts have been similarly reported with success [1,9,34]. In this context, we consistently observed that the *MSC1*-treatment groups had smaller tumors without any detectable metastasis, and accumulated little to no ascites when compared to the MSCs- or *MSC2*-treated groups (Figure 3). Upon staining of the collected ascites, it was evident that there were large tumor aggregates or spheroids present in the MSCs- and *MSC2*-treatment groups but not in the *MSC1* ones. MSC-based therapies of tumors or other diseased organs typically results in very low engraftment by the delivered MSCs. It is established that one hurdle in the translation of MSC-based therapies remains improving their survival in the recipient host [1,9,34].

We used both flow cytometry and immunohistochemical analyses to determine the changes among the treatment groups in the tumor-associated leukocytes (Figures 4 and 5). Here, too, we found changes among the MSC-treated groups as was expected. The CD45+population of cells present in the tumors were more numerous in *MSC1*- and *MSC2*- treatment groups than in MSCs-treated groups. Additionally we measured the greatest number of F4/80+cells in the *MSC1*- treated group compared to the others. The significance of these findings remains to be elucidated. Tumor-associated macrophages (TAMs) are known to be educated from tumor eradicating cells to tumor promoting cells with F4/80 expression potentially changing from one population to the other [35–37]. It will be interesting to determine in future studies whether tumor-associated MSCs and TAMs directly affect each

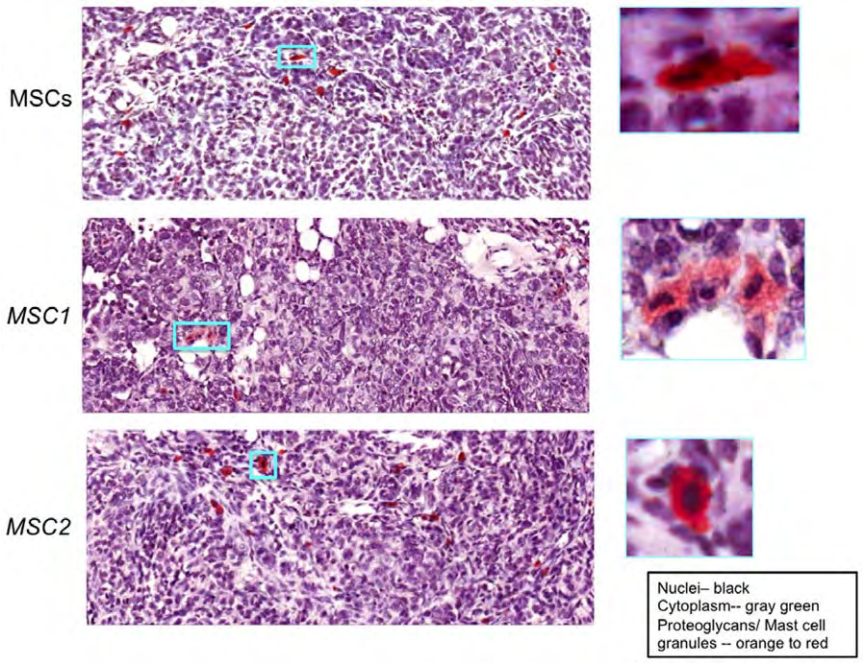

Figure 5. Proteoglycan-rich stained mast cells found in tumor sections from *MSC2*- and MSC-treated tumor groups but mostly degranulated ones found in *MSC1*-treated tumor groups. MOSEC tumors were established in C57BL/6 mice for 4 weeks. MSCs, *MSC1*, or *MSC2* (1×10^6 in 0.5 mL HBSS) were infused IP and the mice were harvested after 65 days. Tumors were excised, fixed, and cut into 5 μM sections by standard methods [7]. Sections were processed for safranin O proteoglycan staining (www.ihcworld.com). Representative micrographs of several MSC-treated tumor sections are included from images obtained from the Aperio ScanScope (200X, Aperio, Vista, CA). The expected color for each tissue element is described in the inset on the lower right hand side. 400X images are included in boxed insets. Data are representative of three independent experiments with at least 6 mice per treatment group.
doi:10.1371/journal.pone.0045590.g005

other and can be "re-educated" from one form to the other following this interaction.

Macrophages, mast cells (MCs), and MSCs also affect ECM proteins, yet another component of the TME important to tumor growth and spread [23,24,30,38]. Thus, the changes in mast cells and collagen (ECM) levels among the MSC-treated tumor groups were measured (Figure 5 and Figure S3). Safranin O stains the proteoglycan-rich granules of mast cells and surprisingly revealed that the MCs of tumor sections of MSCs- and *MSC2*-treated groups were mostly loaded with these granules while the *MSC1*-treated groups were not. Furthermore, we observed localization of the MCs to the stromal compartments of the tumors, which may suggest an association of MCs and the ECM. This association was further implicated by comparison of the safranin O stained sections with those of the Verhoeff-Van Gieson (VVG) collagen stained sections, which revealed mast cells concentrated in areas with the darkest pink/red collagen stained regions (Figure S4). Unexpectedly, we observed the opposite effect of *MSC1* on collagen levels (*in vivo*) than we previously reported for *MSC1* induction alone (*in vitro*) [13]. VVG stained tumor sections from *MSC1*-treated groups had less dark pink/red areas than the other samples, whereas *in vitro MSC1* had the greatest expression of collagen compared to the other samples. These differences may be explained by direct *in vivo* interactions between the MSCs and MCs that were recently discovered and that would be present in the TME but lacking in the *in vitro* setting [25]. Further investigation of the interaction of MCs with MSCs within the TME will have to be added to those of MSCs and macrophages mentioned above. Adding to the complexity of the TME, MSCs, macrophages, and MCs seem to share many properties affecting the secretion of bioactive factors and the tumor immunity [26,39–43].

More detailed analyses are required to complete our understanding of the effect that MSC-based therapies might have on all of the tumor-associated leukocytes including MCs and macrophages. In particular, it would be interesting to begin to dissect the contributions of each leukocyte population in the MSC-affected tumors by using specific mouse knockout models. We also expect that the study of other solid tumor and leukemia models as well as other strains of mice may identify subtle differences in the net effect of the MSC-based therapies that will be useful to our understanding of the TME and its contribution to tumor growth and spread. Important as well will be determining the most effective MSC-based cancer therapy. To this end, the optimal dose, frequency, and timing of the MSC-based therapy need to be determined for each cancer. We are encouraged that the *ex vivo* induced *MSC1* and *MSC2* phenotypes appear to remain stable when re-introduced into various animal disease models and were capable of mediating distinct results even 65 days after just a single MSC injection (Figure 3).

Cell-based therapies are undoubtedly gaining ground given their growing international use, regulatory agency approval (FDA and European Medicines Agency-EMA), billion dollar a year market, and proven efficacy in many human diseases [44]. Among these, *MSC*-based therapies are widely used because MSCs are thus far clinically safe, are easily obtained from adult tissues, can be expanded as well as stored, and are unique in their immune modulating capabilities. Additionally, their proclivity for the tumor microenvironment makes them ideally suited for the directed delivery of anti-cancer payloads. An ideal therapeutic approach for the complex pathology of cancer may be a complementary one

that employs conventional methods to target the cancer cells (seed) combined with MSC-based therapies that target the TME (soil). Finally, the new *MSC1*- and *MSC2*-therapy approach we have identified provides a convenient tool with which to begin to dissect the contribution of MSCs to tumors, and may help resolve some of the surrounding controversies to safely advance the use of MSC-based therapies in many human diseases including cancer.

Materials and Methods

Cells

Bone marrow-derived human MSC (MSCs) used for all studies were obtained from the Tulane Center for Stem Cell Research and Regenerative Medicine, New Orleans, LA or Lonza, Walkersville, MD and are IRB exempt as previously described [13]. MSCs from at least six different human donors were used in these experiments and cultured as previously described [12,45]. All experiments were conducted on MSCs at a passage $\leq$5. HeLa human cervical adenocarcinoma, OVCAR-human ovarian adenocarcinoma, and SKOV3 (SKOV3AB) human ovarian adenocarcinoma were obtained from the American Type Tissue Collection (ATCC, Walkersville, MD). PANC-1 human pancreatic adenocarcinoma, and SKOV3FM were obtained as a gift from Dr. Frank C. Marini (Wake Forest Medical Center, NC and are also commercially available from ATCC, Walkersville, MD). Preparation of MSCs into a pro-inflammatory *MSC1* phenotype or an immunosuppressive *MSC2* phenotype was described previously ([13], patent-pending US 61/391,749).

Animals

Animal care and use was pre-approved by the Tulane University Medical Center Advisory Committee for Animal Resources. 3–7-week-old female C57BL/6J *wt* mice were obtained from Jackson Laboratories (Bar Harbor, ME). The syngeneic mouse model for epithelial ovarian cancer based upon a spontaneously transformed mouse ovarian surface epithelial cell (MOSEC) line ID8 has been previously described [21,46]. ID8 cells were a generous gift from Dr. Katherine F. Roby (Kansas University Medical Center). At approximately 4 weeks post cancer cell introduction and tumor formation, 1×10^6 cells/per mouse of CellTracker fluorescently-labeled wt MSCs, *MSC1*, *MSC2* or mock control was infused IP (Molecular Probes, Life Technologies, Carlsbad, CA) [47]. The ability of the cells to reach their target was measured by flow cytometry analyses of collected tumors 24 hr after the MSC infusions [47]. The 24 hr window was chosen as optimal for MSC engraftment measurements based on previous studies [47]. Mice were monitored daily for changes in weight, morbidity, and mortality. Tumors were measured and at harvest, ascites, tumors and any metastases were weighed and documented as before [7]. Kaplan-Meier survival plots of mice were analyzed by the log rank test (Prism4, GraphPad Software Inc. CA). Greater than 6 mice per sample group was used in each of the experiments.

Flow Cytometry

Single cell suspensions of collected tumors were achieved by the method previously described [32]. Analysis of cell surface markers expressed from the obtained tumor samples was done by multi-color cell surface antibody staining as in that study, or as indicated for the specific cell subsets including anti-CD3, -CD4, -CD8, -CD11b, -CD11c, -CD19, -CD45R, - Ly-6G (Gr-1), and -NKG2D (CD314) [46,48]. Intracellular cytokine antibody staining was achieved after fixation and permeabilization of the cells. Isotype controls and untreated or unstained samples were routinely run in parallel as standard. End point flow cytometry analysis was performed on a BD LSRII analyzer and analyzed with CellQuest software. Data are representative of at least duplicate samples from at least three independent experiments.

Colony Forming Units (CFU) and Tumor Spheroid Assays

CFU assay was performed by culturing human tumor cells (200 cells/well) mixed with conventionally prepared MSCs, *MSC1* or *MSC2* (2 cells/well) at a ratio of 10 cancer cells per MSC and plated in 24-well plates in growth medium supplemented with 10% FBS as indicated. Cultures were grown for 14 days at 37°C in a humidified incubator. Growth medium was changed every 3–4 days. Colonies were visualized by staining with a crystal violet solution (0.5% crystal violet/10% ethanol). The resulting colonies were enumerated by the colony counting macro in ImageJ software. Tumor spheroids were formed by culturing tumor cells (200 cells/well) mixed without any other cells (–) or with CellTracker labeled MSCs, *MSC1* or *MSC2* (20 cells/well) at a ratio of 10 cancer cells per 1 MSC and plated over 1.5% agarose in 96-well plates in growth medium supplemented with 10% FBS as indicated. Cultures were grown for 14 days at 37°C in a humidified incubator. Growth medium was changed every 3–4 days. Micrographs shown represent a 20-fold magnified field of the 96-well plate. CFU and tumor spheroid assays were performed in at least three independent experiments with duplicate wells.

Migration and Invasion Assays

Migration and invasion assays were performed with cells loaded on 3 μM Falcon fluoroblok transwell inserts and allowed 16 hrs in a humified CO2 incubator as described previously [12,20,45]. Transwell migrating and matrigel invading cells were visualized on an inverted fluorescence microscope (Olympus). Image analyses were routinely performed with ImageJ. Data are representative of duplicates in at least three independent experiments.

qPCR

Quantitative Real-Time PCR (qPCR) was carried out as previously described using the following primers pairs [39]: matrix metalloproteinase 1 *(mmp)1*-forward (F) GGA GAT CAT CGG GAC AAC TC*; mmp1*-reverse (R*)*-ACC GGA CTT CAT ATG TCG*; mmp2*-F-CAA GTG GTC CGT GTG AAG TAT G; *mmp2*-R-CGT CAT CGT AGT TGG CTG TG; *mmp3*-F-GAC AAA GGA TAC AAC AGG GAC C; *mmp3*-R-TAT CAG AAA TGG CTG CAT CG; *mmp9*-F-CAA GGA TGG GAA GTA CTG GCG; *mmp9*-R- TCA ACT CAC TCC GGG AAC TC; *mmp13*-F-GAT ACG TTC TTA CAG AAG; *mmp13*-R GAC AAA TCA TCT TCA TCA CC; membrane-type matrix metalloproteinase-1 (*mt-mmp)1*-F-GTC TTC AAG GAG CGC TGG TTC TG *mt-mmp1*-R- TAG CCC GGT TCT ACC TTCA G; *18S rRNA* –F-GAG GGA GCC TGA GAA ACG G, *18S rRNA* -R-GTC GGG AGT GGG TAA TTT GC-3′ (IDT, Coralville, IA). Samples from at least three independent experiments were run in triplicate.

Histology and Immunohistochemistry

The collected ascites samples were spun down on cytospin slides and processed for Diff Quick stain as described (http://www.ihcworld.com/_protocols/special_stains/diff_quick_ellis.htm). Tumors were fixed in 10% formalin solution and embedded in paraffin by standard methods. Sections were cut into 5 μm sections and stained with hematoxylin and eosin (H&E), Verhoeff-Van Gieson (VVG)– elastic fiber/collagen staining and safranin O– proteoglycan staining were performed also as described (www.ihcworld.com). Immunostaining was performed using monoclonal anti-hCAP-18/LL-37, -CD45, -F4/80, and other relevant markers

as before [49]. All stained tissue sections were scanned with the Aperio ScanScope (Aperio, Vista, CA) at an initial magnification of 40X, and images were visualized and captured using the Aperio ImageScope program. Image analyses were routinely performed with ImageJ. For threshold analysis (percent DAB or safranin positive), the images were digitally adjusted to remove background and increase the contrast between the tissue and the background. The RGB images were stacked into separate R, G, B images and threshold determinations were used to digitally highlight all the stained tissue while dismissing the background. Finally, the percent of highlighted pixels (positive cells) was calculated relative to total area of the field. A similar ImageJ analysis method was used to determine collagen positive areas within the VVG stained tumor sections as detailed in http://cardprint.ucsd.edu/CV_Lab_Web_Page/HowToDocs/ImageJProtocol.pdf. Greater than 10 viewing fields were recorded and analyzed after three independent experiments for each sample group.

Statistical Analysis

Data are presented as average +/− standard error of the mean (S.E.M.). Multiple group comparison was performed by one-way analysis of variance (ANOVA) followed by the Bonferroni procedure for comparison of means. Comparison between any two groups was analyzed by the two-tailed Student's t-test or two-way ANOVA (Prism4, GraphPad Software Inc. CA). Values of $P<0.05$ were considered statistically significant.

Supporting Information

Figure S1 MSC1 diminish tumor growth whereas MSC2 favor tumor growth. Tumor spheroids were formed by culturing tumor cells (200 cells/well) mixed without any other cells (–) or with CellTracker green labeled MSCs, *MSC1,* or *MSC2* (20 cells/well) at a ratio of 10 cancer cells per 1 MSC and plated over 1.5% agarose in 96-well plates in growth medium supplemented with 10% FBS as indicated in figure. Cultures were grown for 14 days at 37°C in a humidified atmosphere of 5% carbon dioxide balance air. Growth medium was changed every 3–4 days. Representative micrographs shown represent 20X magnified bright field of the 96-well plate. Cancer cell lines used are: HeLa- human cervical adenocarcinoma, PANC-1- human pancreatic adenocarcinoma, OVCAR-human ovarian adenocarcinoma, SKOV3-human ovarian adenocarcinoma, and MOSEC-murine ovarian surface epithelium carcinoma cells.
(TIF)

Figure S2 MSC1 diminish tumor growth whereas MSC2 favor tumor growth. Fluorescence micrographs corresponding to those bright field micrographs presented in Figure S1. CellTracker green labeled MSCs, *MSC1,* or *MSC2* appear as the brighter spots in the images. It appears that the cells distribute throughout the tumor spheroids–whose shadows are visible in these fluorescence micrographs.
(TIF)

Figure S3 *MSC1*-treated tumor samples have diminished levels of collagen within the TME compared to *MSC2*- and MSC-treated tumor groups. MOSEC tumors were established in C57BL/6 mice for 4 weeks. MSCs, *MSC1,* or *MSC2* (1×10^6 in 0.5 mL HBSS) were infused IP and the mice were harvested after 65 days. Tumors were excised, fixed, and cut into 5 μM sections by standard methods [7]. Sections were processed for Verhoeff-Van Gieson (VVG) elastic fiber/collagen staining (www.ihcworld.com). Representative micrographs of several MSC-treated tumor sections are included from images obtained from the Aperio ScanScope (40X, Aperio, Vista, CA). The expected color for each tissue element is described in the inset on the lower right hand side. 80X images are included in boxed insets. Data are representative of three independent experiments with at least 6 mice per treatment group.
(TIF)

Figure S4 Co-localization of tumor associated mast cells with collagen. MOSEC tumors were established in C57BL/6 mice for 4 weeks. MSCs, *MSC1,* or *MSC2* (1×10^6 in 0.5 mL HBSS) were infused IP and the mice were harvested after 65 days. Tumors were excised, fixed, and cut into 5 μM sections by standard methods [7]. Sections were processed for Verhoeff-Van Gieson (VVG) elastic fiber/collagen staining (left panels) or for safranin O proteoglycan staining (right panels, www.ihcworld.com). Representative micrographs of several MSC-treated tumor sections are included from images obtained from the Aperio ScanScope (40X, Aperio, Vista, CA). Yellow arrows indicate comparable sections among the tumor tissue sections. Data are representative of three independent experiments with at least 6 mice per treatment group.
(TIF)

Acknowledgments

We would like to thank Dr. Frank C. Marini (Wake Forest Baptist Medical Center, NC) for generously providing the SKOV3 and PANC-1 cells and numerous discussions that guided this work. We thank Dr. Leann Myers (Biostatistics & Bioinformatics Department, Tulane University) for help with the statistical analysis of our data. We are also grateful for the technical assistance provided by Sophia and Anna Scandurro.

Author Contributions

Conceived and designed the experiments: RSW AMB. Performed the experiments: RSW SLH AMB. Analyzed the data: RSW SLH AMB. Contributed reagents/materials/analysis tools: RSW SLH AMB. Wrote the paper: RSW AMB.

References

1. Salem HK, Thiemermann C (2010) Mesenchymal stromal cells: current understanding and clinical status. Stem Cells 28: 585–596.
2. Tolar J, Le Blanc K, Keating A, Blazar BR (2010) Concise review: hitting the right spot with mesenchymal stromal cells. Stem Cells 28: 1446–1455.
3. Waterman RS, Betancourt AM (2012) The role of mesenchymal stem cells in the tumor microenvironment: InTech. http://www.intechopen.com/books/tumor-microenvironment-and-myelomonocytic-cells/the-role-of-mesenchymal-stem-cells-in-the-tumor-microenvironment.
4. Klopp AH, Gupta A, Spaeth E, Andreeff M, Marini F 3rd (2010) Dissecting a Discrepancy in the Literature: Do Mesenchymal Stem Cells Support or Suppress Tumor Growth? Stem Cells.
5. Klopp AH, Gupta A, Spaeth E, Andreeff M, Marini F 3rd (2011) Concise review: Dissecting a discrepancy in the literature: do mesenchymal stem cells support or suppress tumor growth? Stem Cells 29: 11–19.
6. Kidd S, Spaeth E, Klopp A, Andreeff M, Hall B, et al. (2008) The (in) auspicious role of mesenchymal stromal cells in cancer: be it friend or foe. Cytotherapy 10: 657–667.
7. Coffelt SB, Marini FC, Watson K, Zwezdaryk KJ, Dembinski JL, et al. (2009) The pro-inflammatory peptide LL-37 promotes ovarian tumor progression through recruitment of multipotent mesenchymal stromal cells. Proc Natl Acad Sci U S A 106: 3806–3811.
8. Karnoub AE, Dash AB, Vo AP, Sullivan A, Brooks MW, et al. (2007) Mesenchymal stem cells within tumour stroma promote breast cancer metastasis. Nature 449: 557–563.
9. Rayment EA, Williams DJ (2010) Concise review: mind the gap: challenges in characterizing and quantifying cell- and tissue-based therapies for clinical translation. Stem Cells 28: 996–1004.

10. von Bahr L, Batsis I, Moll G, Hagg M, Szakos A, et al. (2012) Analysis of Tissues Following Mesenchymal Stromal Cell Therapy in Humans Indicate Limited Long-Term Engraftment and No Ectopic Tissue Formation. Stem Cells.
11. Coffelt SB, Scandurro AB (2008) Tumors sound the alarmin(s). Cancer Res 68: 6482–6485.
12. Zwezdaryk KJ, Coffelt SB, Figueroa YG, Liu J, Phinney DG, et al. (2007) Erythropoietin, a hypoxia-regulated factor, elicits a pro-angiogenic program in human mesenchymal stem cells. Exp Hematol 35: 640–652.
13. Waterman RS, Tomchuck SL, Henkle SL, Betancourt AM (2010) A new mesenchymal stem cell (MSC) paradigm: polarization into a pro-inflammatory MSC1 or an Immunosuppressive MSC2 phenotype. PLoS One 5: e10088.
14. Waterman RS, Jenny M, Bobby DN, Anna ES, Aline MB (2012) Anti-Inflammatory Mesenchymal Stem Cells (MSC2) Attenuate Symptoms of Painful Diabetic Peripheral Neuropathy. Stem Cells Translational Medicine: 557–565.
15. Mantovani A, Sozzani S, Locati M, Allavena P, Sica A (2002) Macrophage polarization: tumor-associated macrophages as a paradigm for polarized M2 mononuclear phagocytes. Trends Immunol 23: 549–555.
16. Martinez FO, Gordon S, Locati M, Mantovani A (2006) Transcriptional profiling of the human monocyte-to-macrophage differentiation and polarization: new molecules and patterns of gene expression. J Immunol 177: 7303–7311.
17. Mosser DM, Zhang X (2008) Activation of murine macrophages. Curr Protoc Immunol Chapter 14: Unit 14 12.
18. Mosser DM, Edwards JP (2008) Exploring the full spectrum of macrophage activation. Nat Rev Immunol 8: 958–969.
19. Mantovani A, Sica A, Locati M (2007) New vistas on macrophage differentiation and activation. Eur J Immunol 37: 14–16.
20. Coffelt SB, Tomchuck SL, Zwezdaryk KJ, Danka ES, Scandurro AB (2009) Leucine leucine-37 uses formyl peptide receptor-like 1 to activate signal transduction pathways, stimulate oncogenic gene expression, and enhance the invasiveness of ovarian cancer cells. Mol Cancer Res 7: 907–915.
21. Roby KF, Taylor CC, Sweetwood JP, Cheng Y, Pace JL, et al. (2000) Development of a syngeneic mouse model for events related to ovarian cancer. Carcinogenesis 21: 585–591.
22. Ribatti D, Nico B, Finato N, Crivellato E (2011) Tryptase-positive mast cells and CD8-positive T cells in human endometrial cancer. Pathol Int 61: 442–444.
23. Murdoch C, Muthana M, Coffelt SB, Lewis CE (2008) The role of myeloid cells in the promotion of tumour angiogenesis. Nat Rev Cancer 8: 618–631.
24. Navi D, Saegusa J, Liu FT (2007) Mast cells and immunological skin diseases. Clin Rev Allergy Immunol 33: 144–155.
25. Brown JM, Nemeth K, Kushnir-Sukhov NM, Metcalfe DD, Mezey E (2011) Bone marrow stromal cells inhibit mast cell function via a COX2-dependent mechanism. Clin Exp Allergy 41: 526–534.
26. Bianchi G, Borgonovo G, Pistoia V, Raffaghello L (2011) Immunosuppressive cells and tumour microenvironment: focus on mesenchymal stem cells and myeloid derived suppressor cells. Histol Histopathol 26: 941–951.
27. Djouad F, Plence P, Bony C, Tropel P, Apparailly F, et al. (2003) Immunosuppressive effect of mesenchymal stem cells favors tumor growth in allogeneic animals. Blood 102: 3837–3844.
28. Khakoo AY, Pati S, Anderson SA, Reid W, Elshal MF, et al. (2006) Human mesenchymal stem cells exert potent antitumorigenic effects in a model of Kaposi's sarcoma. J Exp Med 203: 1235–1247.
29. Shinagawa K, Kitadai Y, Tanaka M, Sumida T, Kodama M, et al. (2010) Mesenchymal stem cells enhance growth and metastasis of colon cancer. Int J Cancer 127: 2323–2333.
30. Gialeli C, Theocharis AD, Karamanos NK (2010) Roles of matrix metalloproteinases in cancer progression and their pharmacological targeting. FEBS J 278: 16–27.
31. Cubillos-Ruiz JR, Rutkowski M, Conejo-Garcia JR (2010) Blocking ovarian cancer progression by targeting tumor microenvironmental leukocytes. Cell Cycle 9: 260–268.
32. Nesbeth Y, Scarlett U, Cubillos-Ruiz J, Martinez D, Engle X, et al. (2009) CCL5-mediated endogenous antitumor immunity elicited by adoptively transferred lymphocytes and dendritic cell depletion. Cancer Res 69: 6331–6338.
33. Prockop DJ, Youn Oh J (2011) Mesenchymal Stem/Stromal Cells (MSCs): Role as Guardians of Inflammation. Mol Ther.
34. Singer NG, Caplan AI (2011) Mesenchymal stem cells: mechanisms of inflammation. Annu Rev Pathol 6: 457–478.
35. Condeelis J, Pollard JW (2006) Macrophages: obligate partners for tumor cell migration, invasion, and metastasis. Cell 124: 263–266.
36. Baay M, Brouwer A, Pauwels P, Peeters M, Lardon F (2011) Tumor cells and tumor-associated macrophages: secreted proteins as potential targets for therapy. Clin Dev Immunol 2011: 565187.
37. Sica A, Bronte V (2007) Altered macrophage differentiation and immune dysfunction in tumor development. J Clin Invest 117: 1155–1166.
38. Ingman WV, Wyckoff J, Gouon-Evans V, Condeelis J, Pollard JW (2006) Macrophages promote collagen fibrillogenesis around terminal end buds of the developing mammary gland. Dev Dyn 235: 3222–3229.
39. Coffelt SB, Hughes R, Lewis CE (2009) Tumor-associated macrophages: Effectors of angiogenesis and tumor progression. Biochim Biophys Acta 1796: 11–18.
40. Coussens LM, Werb Z (2002) Inflammation and cancer. Nature 420: 860–867.
41. Fidler IJ (2003) The pathogenesis of cancer metastasis: the 'seed and soil' hypothesis revisited. Nat Rev Cancer 3: 453–458.
42. Rabinovich GA, Gabrilovich D, Sotomayor EM (2007) Immunosuppressive strategies that are mediated by tumor cells. Annu Rev Immunol 25: 267–296.
43. Strausberg RL (2005) Tumor microenvironments, the immune system and cancer survival. Genome Biol 6: 211.
44. Mason C, Brindley DA, Culme-Seymour EJ, Davie NL (2011) Cell therapy industry: billion dollar global business with unlimited potential. Regen Med 6: 265–272.
45. Tomchuck SL, Zwezdaryk KJ, Coffelt SB, Waterman RS, Danka ES, et al. (2008) Toll-like receptors on human mesenchymal stem cells drive their migration and immunomodulating responses. Stem Cells 26: 99–107.
46. Liu Y, Zeng B, Zhang Z, Zhang Y, Yang R (2008) B7-H1 on myeloid-derived suppressor cells in immune suppression by a mouse model of ovarian cancer. Clin Immunol 129: 471–481.
47. Ohtaki H, Ylostalo JH, Foraker JE, Robinson AP, Reger RL, et al. (2008) Stem/progenitor cells from bone marrow decrease neuronal death in global ischemia by modulation of inflammatory/immune responses. Proc Natl Acad Sci U S A 105: 14638–14643.
48. Yang R, Cai Z, Zhang Y, Yutzy WH, Roby KF, et al. (2006) CD80 in immune suppression by mouse ovarian carcinoma-associated Gr-1+CD11b+ myeloid cells. Cancer Res 66: 6807–6815.
49. Coffelt SB, Waterman RS, Florez L, Honer zu Bentrup K, Zwezdaryk KJ, et al. (2008) Ovarian cancers overexpress the antimicrobial protein hCAP-18 and its derivative LL-37 increases ovarian cancer cell proliferation and invasion. Int J Cancer 122: 1030–1039.